Interactions Between Canine Plasminogen and ANS: Structural Insight into the Binding Determinants of a Fluorescent Probe

David Carter

A Thesis

in

The Department

of

Chemistry and Biochemistry

Presented in Partial Fulfillment of the Requirements
for the Degree of Master of Science (Chemistry) at
Concordia University
Montreal, Quebec, Canada

September 2004

Your file Votre référence
ISBN: 0-612-94666-5
Our file Notre référence
ISBN: 0-612-94666-5

Abstract

Interactions Between Canine Plasminogen and ANS: Structural Insight into the Binding Determinants of a Fluorescent Probe

David Carter

The canine variant of the serum protein, plasminogen (DPgn) binds the fluorescent molecule, 8-anilino-1-naphthalene sulfonate (ANS). Binding is pronounced at low pH, as witnessed by steady-state fluorescence, native PAGE and isothermal titration calorimetry. At pH 6.3 ANS binding occurs, but with a largely diminished magnitude. Binding occurs at multiple sites. A strong site binds ANS with a K_a of 3.3 x 10^4 M^{-1}. Two weaker sites were observed with K_a's of 6.2 x 10^3 M^{-1} and 360 M^{-1} respectively. ANS binds equally well to both the closed and opened conformations of DPgn at pH 3.0. Enhanced binding at low pH is accompanied with changes in protein flexibility as monitored by sedimentation velocity analysis. Changes in frictional ratios were observed indicating an increased flexibility for both conformations of DPgn at pH 3.0 compared to pH 6.3. This finding was confirmed from the observation of altered near UV circular dichroism spectra of the protein at low pH. Taken together, the data indicate that ANS may be binding to a pH induced molten globule state of DPgn. Binding sites for ANS were localized within kringle domains as well as the proteolytic domain. However, it is unlikely that binding occurs within the lysine binding sites of each respective kringle.

Acknowledgements:

I would like to thank my thesis advisor, Dr. Jack Kornblatt, for his aid in helping me achieve the realization of this work. I would also like to thank him for his patience in seeing me through this project.

I would like to thank my committee members, Dr. Ann English, Dr. Christine Dewolf and Dr. Justin Powlowski for reviewing the course of my progress and taking the time to appreciate this work.

I would like to thank my parents Percy and Orangie Carter for their encouragement and support. They have always been there for me and are simply the best.

I would like to thank my girlfriend, Leila Kristiansen who has also encouraged me and listened to my enthusiastic speculations on protein structure. Without her, I'd be lost.

I wish to thank my family and friends who have given me many reasons to laugh and even cry when it's time for them to go away.

Finally, I wish to thank everyone else in the Dept. of Chemistry and Biochemistry at Concordia University. They have provided me with continual support and have encouraged me to further develop my knowledge within the field of biochemistry.

Table of Contents:

List of Figures:

List of Tables:

List of Abbreviations Used:

ANS:	8-anilino-1-naphthalene sulfonate
Pgn:	Plasminogen
Glu-Pgn:	Variant of plasminogen containing N-terminal glutamic acid
Lys-Pgn:	Variant of plasminogen containing N-terminal lysine
Pm:	Plasmin
Glu-Pm:	Variant of plasmin containing N-terminal glutamic acid
Lys-Pm:	Variant of plasmin containing N-terminal lysine
DPgn:	Canine variant of plasminogen
HPgn:	Human variant of plasminogen
PAGE:	Polyacrylamide Gel Electrophoresis
SDS:	Sodium Dodecyl Sulphate
CD:	Circular Dichroism Spectroscopy
AUC:	Analytical Ultracentrifugation
ITC:	Isothermal Titration Calorimetry
t-PA:	Tissue Type Plasminogen Activator
u-PA:	Urokinase Plasminogen Activator
NTP:	N-terminal Peptide
K:	Kringle
LBS:	Lysine Binding Site
BSA:	Bovine Serum Albumin
6-AH:	6-aminohexanoate
OD_{280}:	Optical Density at 280 nm

1.0 Introduction

This thesis focuses on the interactions between the canine variant of the serum protein plasminogen and ANS, a fluorescent probe. The use of ANS as a probe allows one to examine protein tertiary structure. In doing so, it yields information pertaining to local hydrophobicity within a global protein fold. Before these interactions are discussed in detail, a brief introduction of the system studied will be presented. In this regard, plasminogen will be examined with respect to its structure, its *in vivo* activities and the biochemistry of its activation. The focus will then shift to the use of ANS as a fluorescent probe. The usefulness of ANS as a probe of protein structure will be discussed. Finally the questions one may ask from the use of ANS as a reporter molecule will be considered along with a brief history of some of these uses.

1.1 Plasminogen: Biological Function

Plasminogen (Pgn) is a mammalian serum protein produced by liver hepatocytes. Under normal circumstances it reaches blood concentrations as high as 2 μM (Takada, Takada 1988). It is a zymogen, that is to say it circulates in an inactive state until encountering agents capable of converting it to the protease plasmin. Activation of Pgn is complicated and is discussed in greater detail below. Upon activation, the serine protease, plasmin (Pm), is formed. Plasmin, in turn, has been implicated in the regulation of many disparate biological functions. A few of these will now be examined in greater detail.

1.1.1 Fibrinolysis

Primary among the many functions of Pm activity is the regulation of fibrinolysis. Fibrinolysis refers to the dissolution of a fibrin based blood clot. This activity results from a Pm mediated cleavage of the clot, resulting in the release of fibrin proteolytic fragments. Fibrinolysis occurs in response to Pgn activation by the various Pgn activators.

The process of fibrinolysis begins after formation of the fibrin based blood clot. Under most circumstances, clot formation is desirable and leads toward wound recovery. In this manner, wound induced trauma initiates clot formation via the blood coagulation cascade. While not discussed in detail here, this cascade ultimately results in the formation of a polymerized fibrin clot from precursor fibrinogen monomers. Thrombin is the terminal enzyme of this cascade and is responsible for processing fibrinogen. Its activity converts fibrinogen monomers into the polymerized array constituting a clot (Nieuwenhuizen 2001).

Problems arise with serious health consequences when clots become dislodged from their loci of origin. In such cases, they freely circulate throughout the bloodstream, ultimately encountering constricted blood vessels. Occurrence of such an event blocks proper blood flow through the constricted blood vessel. Stroke results if the errant blood clot localizes in the brain, while myocardial infarct (heart attack) occurs if it localizes within the heart. Figure 1 illustrates a schematic of this process.

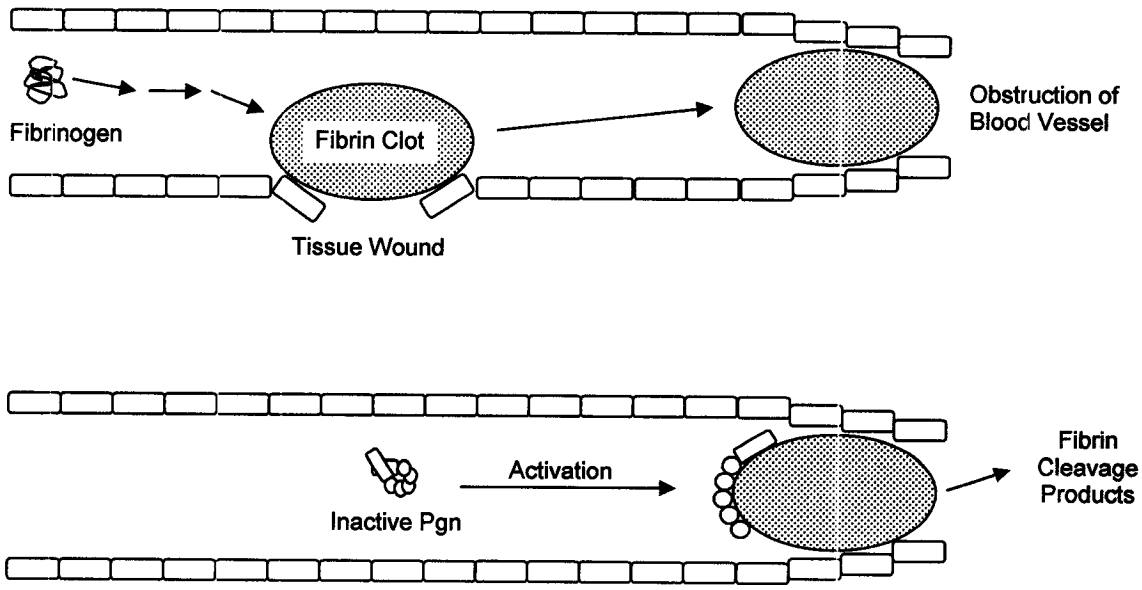

Figure 1: Plasmin and the Fibrinolytic Cycle. Top Panel: The fibrinolytic cycle begins with the formation of a coagulated fibrin clot at the site of an endothelial tissue wound (Left). If the clot becomes dislodged from its locus of origin it can obstruct blood flow at a constricted vessel (Right). Bottom Panel: Activation of plasminogen on a fibrin surface induces plasmin activity followed by clot dissolution. Endothelial cells constituting a blood vessel are represented as rectangles.

The ability of Pm to digest fibrin has stimulated an immense focus on the development of Pgn activators. To illustrate this, it is estimated that the economic impact of stroke and heart attack related health care costs will amount to approximately 75 billion dollars for the American population in 2004 (American Heart Association 2004). Development of more efficient Pgn activators could help reduce these costs while saving lives in the process. Aside from the desirable fibrinolytic properties of Pgn, are other perhaps equally important activities.

Being a proteolytic enzyme, Pm is not surprisingly involved in a broad range of secondary activities. These activities include activation of extracellular proteases, tissue modeling, degradation of the extracellular matrix, prohormone processing, and pathogen invasion. The family of activities represented by Pgn activation is illustrated in Figure 2 (adapted from (Parry et al. 2000)).

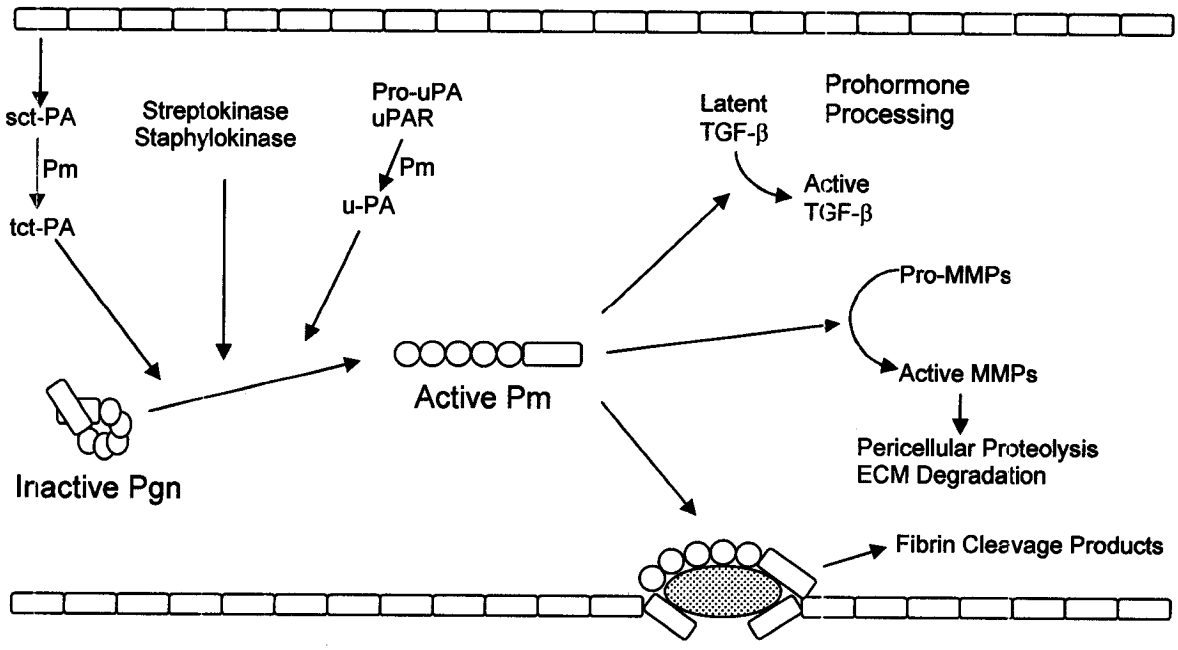

Figure 2: Physiological Processes Involving Plasminogen Activation. Activation of plasminogen by plasminogen activators results in the regulation of many distinct physiological events. Abbreviations: sct-PA – single chain tissue plasminogen activator, tct-PA – active two chain tissue plasminogen activator, uPAR – urokinase plasminogen activator receptor, u-PA – active urokinase plasminogen activator, TGF-β - tissue growth factor β, MMPs – matrix metalloproteases, ECM- extracellular matrix. The figure is not drawn to scale. For example, while a fibrin clot can be anywhere from 20 microns to many centimeters in length, a molecule of Pgn is on the order of 40 nm. Similarly, a single endothelial cell is several microns in length.

1.1.2 Activation of Extracellular Proteases

Zymogen activation is a secondary activity of Pgn. Activated zymogens in turn process various other physiological substrates. For example, Pm activated matrix metalloproteases are involved in their own array of activities including degradation of the extracellular matrix and pericellular proteolysis (Parry et al. 2000). The latter activity can lead to subsequent zymogen activation thus establishing a complex regulatory circuit. This activity also promotes cell migration. For example, cleavage of cellular adhesion proteins that connect adjacent cells within the vasculature allows the cells to migrate freely throughout the bloodstream to locations where they are needed. Tissue modeling is a process involving such activities.

1.1.3 Prohormone Processing

In an analogous manner to zymogen activation, Pm has been shown to activate prohormones (Miles et al. 2003). In this manner, Pm is implicitly involved in endocrine function. For example, when associated with neuroendocrine cells, Pm has shown the ability to produce active transforming growth factor (Parry et al. 2000).

1.1.4 Pathogen Invasion

Not all activities possessed by Pm are so benign. Pathogenic bacteria have evolved the ability to recruit these proteolytic activities to aid in host invasion (Gladysheva et al. 2003). For example, *Streptococci* bacteria produce a well known Pgn activator, streptokinase. Production of this activator aids in the invasive potential of the species. Another species recruiting this ability includes *Y. pestis*, the bacterium responsible for three human pandemics of the plague (Soldeinde O.A., Goguen J.D. 1989). Tumor cells have also been shown to recruit Pm proteolytic activity to aid in growth across surrounding tissue (Miles et al. 2003).

1.2 Plasminogen Activation

All of the aforementioned activities rely upon the ability of the various Pgn activators to efficiently activate Pgn. It is therefore not surprising that there has been such an interest focused upon achieving an understanding of the events leading to the activation of Pgn. In the following, Pgn activation is examined in greater detail. Activators and effectors of activation will be discussed. In doing so, the underlying importance of Pgn conformational flexibility will be realized.

Generally, the activation of Pgn occurs by one of two distinct routes (Parry et al. 2000). In the first route, two chained Pm is formed from its single chain precursor, Pgn. In the second route, a catalytically active single chain Pm is generated upon complex formation with exogenous activators. In the first route Pgn activation occurs via proteolytic processing of a specific activation bond while in the second route no such processing occurs. The endogenous route towards Pgn activation is considered first.

1.2.1 Endogenous Plasminogen Activation

Plasminogen activation is of central importance in the regulation of fibrinolysis. Depicted in Figure 2 are some of the various known activities of Pgn along with various activators of Pgn. Of these, two well characterized Pgn activators include tissue type Plasminogen activator (t-PA) and urokinase plasminogen activator (u-PA). Both activators proteolytically cleave Pgn and are considered next in the context of fibrinolysis.

Endogenous Pgn activation occurs first upon binding of Pgn to the surface of the fibrin clot. Binding to fibrin facilitates a conformational change such that the protein adopts a more extended conformation (Nieuwenhuizen 2001). This extended conformation substantially differs from the more compact conformation of freely circulating Pgn.

The conformational change induced upon binding to fibrin increases exposure of a scissile activation bond within the proteolytic domain of Pgn. Cleavage of this bond by either t-PA or u-PA results in a molecular rearrangement of the catalytic residues within the Pgn active site, to yield Pm (Wang et al. 2000). In Human Plasminogen (HPgn), the

activation bond is located at Arg561-Val562, within the proteolytic domain. Cleavage of this bond does not liberate the previously connected fragments. Rather, the two fragments remain connected by a single disulfide bond.

It is important to note that cleavage of the activation bond in Pgn is enough to generate only a functional active site. Despite this functionality, it is not this form of Pm which is observed in the vast majority of activities noted. Rather, a modified form of Pm known as Lys-Pm is primarily responsible for the noted activities. This is reflected in the observation that catalytic efficiency associated with Lys-Pgn activation is roughly 10-fold that of Glu-Pgn (Wallen 1978;Fredenburgh, Nesheim 1992).

The primary active form of Pm contains an N-terminal lysine residue and is thus named Lys-Pm. This form differs from native Pgn whose N-terminal residue is glutamic acid. Illustrated in Figures 3 and 4 are the different forms taken by Pgn which are discussed in detail here. The nomenclature pertaining to all different forms of Pgn is listed in Figure 3 while the nomenclature pertaining to the activation of Pm is listed in Figure 4. The nomenclature is essentially identical for both Pgn and Pm with the exception that Pm refers to activated Pgn whose activation bond has been cleaved.

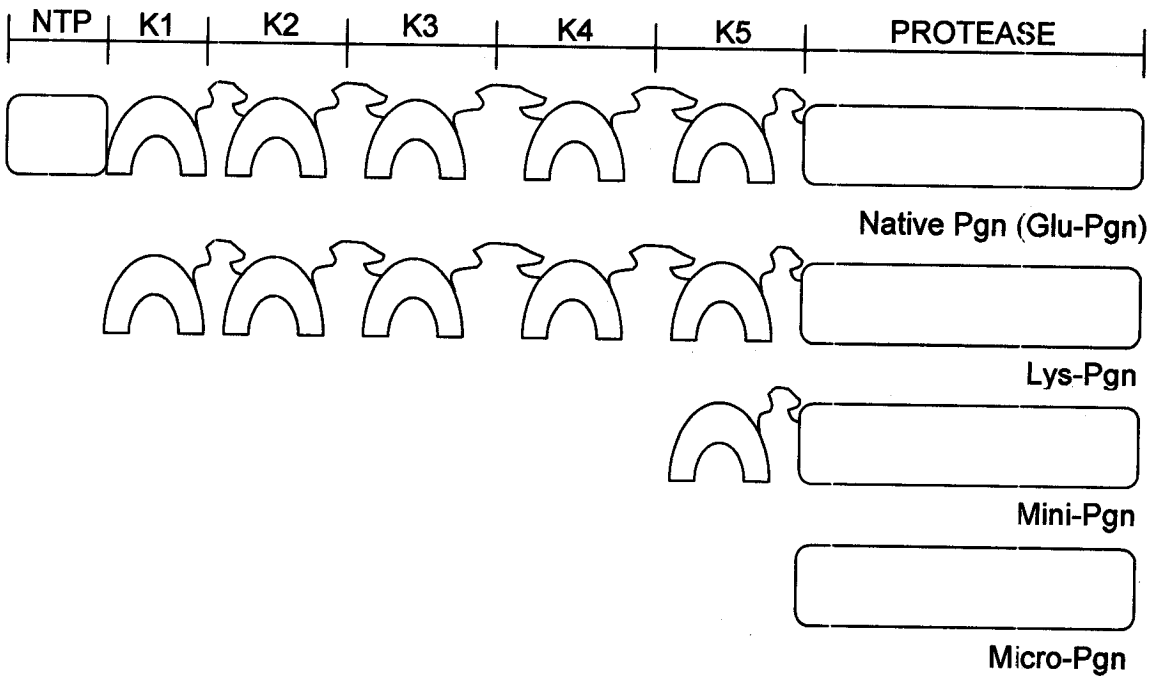

Figure 3: Various Forms of Plasminogen. Shown are the various forms observed of plasminogen. A domain map at the top of the figure illustrates the modular constituents of the holoprotein. Native human plasminogen (Glu-Pgn) contains 790 amino acids with an N-terminal glutamic acid. Cleavage at Lys-77 yields Lys-Pgn. Mini plasminogen contains only kringle 5 and the proteolytic domain. Micro plasminogen contains only the proteolytic domain. Curved lines between domains represent linkers of variable length. Abbreviations: NTP: N-terminal Peptide; K1-K5: Kringles 1-5

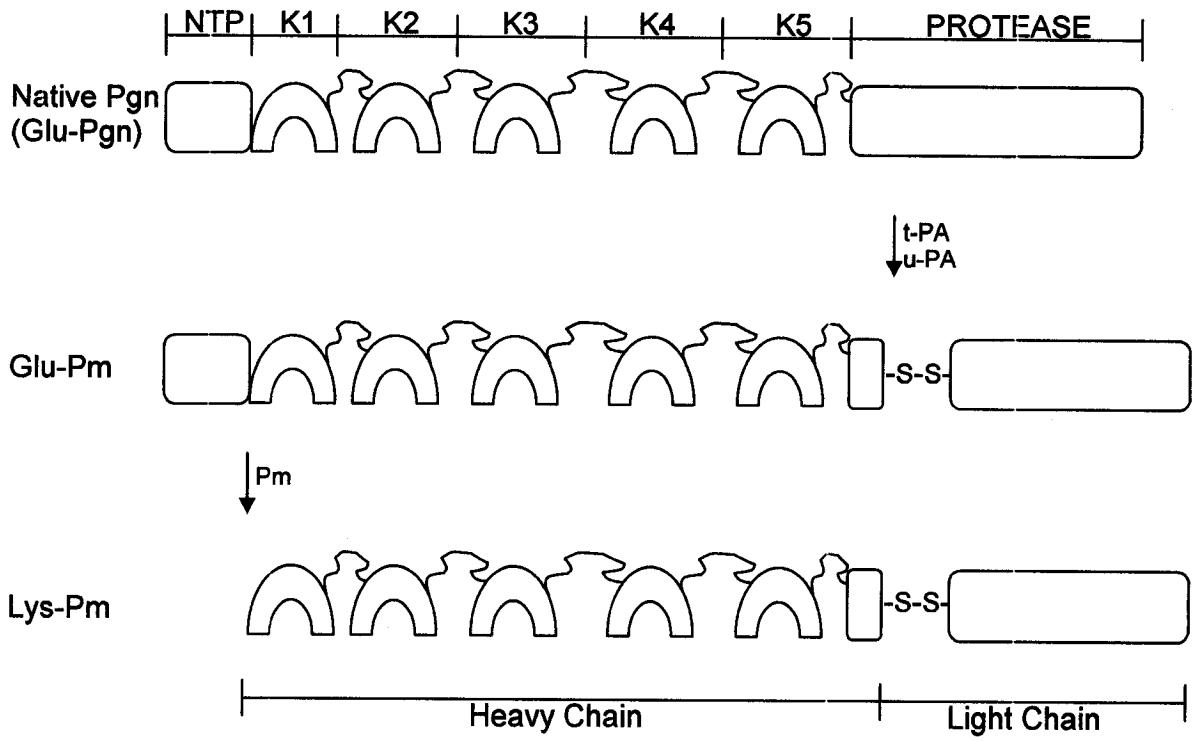

Figure 4: Nomenclature Associated with Plasminogen Activation. (Top) Glu-Pgn is the inactive form of the zymogen. (Middle) Cleavage of the Arg561-Val562 activation bond by plasminogen activators yields Glu-Pm. Glu-Pm contains two chains; a heavy chain consisting of the N-terminus to Arg561 and a light chain consisting of Val562 to the C-terminus. (Bottom) Conversion to Lys-Pm occurs upon a Pm mediated cleavage of Glu-Pm at Lys77, liberating the free N-terminal peptide.

Production of Lys-Pm follows the activator mediated cleavage of the scissile activation bond. The production of Lys-Pm, in turn, occurs by a Pm mediated cleavage at the carboxy terminal side of residues Lys62, Arg68, or Lys77 (Miles et al. 2003). This cleavage results in liberation of the approximately 80 residue N-terminal peptide (NTP) comprised of residues Glu1 to either of the residues preceding the cleavage site (Figure 4).

Pm cannot autoactivate nearby Pgn molecules by direct cleavage of the activation bond. Rather, it can stimulate activation by cleavage of the NTP from neighboring Pgn molecules to yield Lys-Pgn. The newly formed Lys-Pgn is subsequently more readily activated to Lys-Pm than its Glu-Pgn variant.

1.2.2 Exogenous Plasminogen Activation

The second route of Pgn activation occurs in an entirely different manner than does the endogenous pathway. This pathway is exploited by invasive pathogenic bacteria upon entry into the bloodstream. Virulent bacterial species produce Pgn activators to aid in dissemination within the bloodstream upon wound formation. In this scenario, the bacteria are transmitted from the bite of an infected species, i.e. a flea bite, whereupon Pgn activators prevent fibrin formation at the wound location (Sodeinde, Goguen 1989). Doing so decreases the likelihood that fibrin formation would create a physical barrier preventing entry into the host's bloodstream. Two examples of such activators include streptokinase produced from *streptococcus* and staphylokinase produced from *staphylococcus*.

Activation of Pgn from the known exogenous bacterial activators proceeds upon formation of a stoichiometric functional complex between the activators and a molecule of Pgn. Formation of this complex causes two major changes to occur. First, active site residues within the proteolytic domain undergo a rearrangement. This rearrangement results in the formation of a functional active site (Parry et al. 2000;Wang et al. 2000). Second, activation shifts the substrate specificity of the activator-Pgn complex towards that of the activation loop contained within the Pgn proteolytic domain.

The functional active site of the activator-Pgn complex differs from that of free Pgn. The active site located within the proteolytic domain of Pgn contains catalytic residues improperly aligned to yield a functional active site. In HPgn, these residues include His603, Asp646 and Ser741 constituting the classical catalytic triad required of all serine proteases.

Binding of Pgn to streptokinase or staphylokinase ultimately causes a rearrangement of the catalytic triad within the Pgn proteolytic domain. In Pgn, the catalytic triad residues are improperly aligned due to a hydrogen bond between His586 and Asp740 (Peisach E. et al. 1999). This hydrogen bond prevents proper formation of the oxyanion hole, a critical determinant for the activity of all serine proteases. In the Pgn-streptokinase complex, this hydrogen bond is disrupted, yielding a functional oxyanion hole along with proper positioning of the catalytic triad.

Plasminogen substrate specificity is switched upon binding bacterial activators. In this regard the specificity of the Pgn substrate binding pocket favors that of the Pgn activation bond (Parry et al. 2000). This differs from endogenous activation where nascent Pm exhibits a substrate preference for physiological substrates (i.e. fibrin) or the NTP of Pgn, but not the activation bond of Pgn. Thus, in the exogenous Pgn activation pathway, binding to a bacterial activator bestows catalytic activity favoring the cleavage of the Pgn activation bond to an otherwise inactive zymogen. This is the cumulative result of altered substrate specificity coupled to the realigned catalytic triad.

1.2.3 Effectors of Plasminogen Activation

Despite the efficient activation afforded by the activators previously discussed, effectors have been discovered which modulate Pgn activation kinetics. In particular, many small molecules have been shown to modulate these kinetics. Examples include lysine analogs, p-aminobenzamidine and various inorganic ions (Markus G. 1996). Effectors often exert different effects on activation rates where they may both stimulate or inhibit activation. For example, lysine analogs exhibit a stimulatory effect on

endogenous activation pathways while inorganic anions oppose this effect (Urano et al. 1987). Lysine analogs, in particular, have played a large role leading to the current understanding of Pgn activation. They are discussed next.

1.2.3.1 Lysine Analogs and Plasminogen Activation:

It has long been established that lysine analogs are effective modulators of Pgn activation rates. One such analog, 6-aminohexanoate (6-AH) (Figure 5) has often been used to illustrate this point. Activation rates catalyzed by u-PA have been showed to double in the presence of 6-AH (Urano et al. 1987).

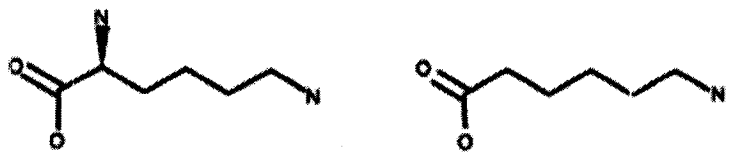

Lysine 6-aminohexanoate

Figure 5: Effectors of Plasminogen Activation: Proteins containing N-terminal lysine residues such as fibrin stimulate plasminogen activation. Lysine analogs such as 6-aminohexanoate (6-AH) also stimulate plasminogen activation.

The mechanism whereby lysine analogs stimulate Pgn activation involves large conformational changes similar to those resulting from binding to fibrin. These changes require binding sites for the analogs. Four such binding sites are found in HPgn. Binding of lysine and lysine analogs at these sites facilitate the conformational change, ultimately yielding a more extended conformation of Pgn. In fact, the presence of lysine binding sites is a requirement for interactions between Pgn and many of its known substrates. These substrates often possess N-terminal lysines facilitating the interactions.

Conformational changes induced by the binding of lysine and lysine analogs are of central importance in understanding the activation of Pgn. The conformational transition will be examined in greater detail later. This transition is intimately related to Pgn structure.

1.3 General Considerations of Plasminogen Structure

The human variant of Pgn is a 90 kDa glycoprotein containing approximately 790 amino acids (Figure 6). Two glycosylated variants are commonly observed. Variant one is diglycosylated containing both a mannose type carbohydrate with 10 to 11 linked monosaccharide substituents attached to Asn288 and a galactose containing trisaccharide attached to Thr345 (Castellino 1984;Miyashita et al. 1988). Variant two is monoglycosylated containing only the trisaccharide attached to Thr345. Additional heterogeneity is observed due to a variable extent of sialic acid content. Regardless, all variants observed for Pgn are similar with respect to their biological functions and such differences will not be considered further.

Figure 6: Primary Structure of Human Plasminogen. The primary sequence of human plasminogen is illustrated. The activation bond is indicated with an opened triangle. The modular composition is evident from the figure. Abbreviations: PAN: N-terminal module that is cleaved upon production of Lys-Pgn. Taken with permission from the website of Dr. Miguel Llinas (Llinas 2004).

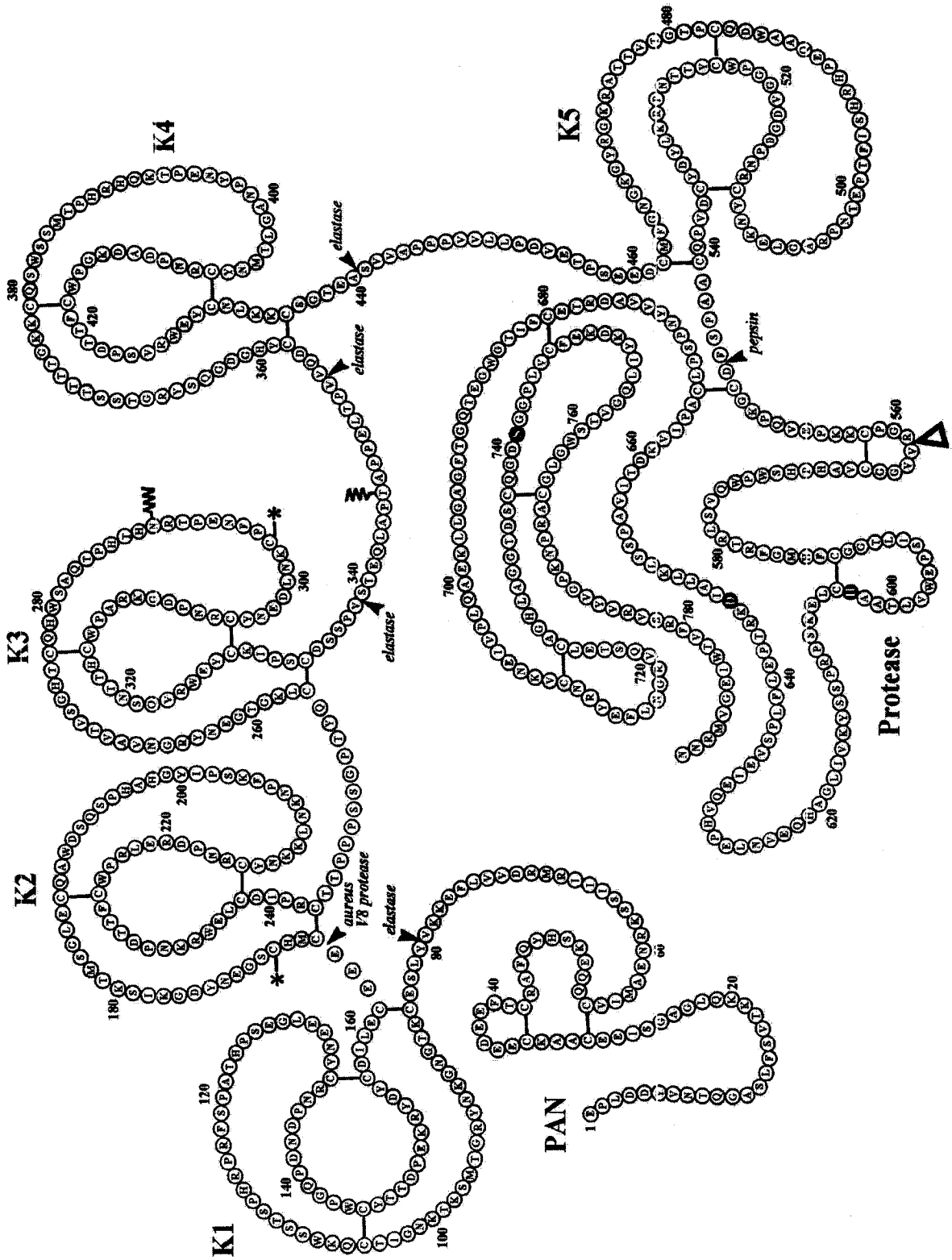

1.3.1 Plasminogen Topology

Plasminogen is a modular protein comprised of seven domains. A schematic of HPgn topology is illustrated in Figure 6. The overall structure includes an N-terminal peptide followed by five homologous peptides known as kringle domains. The C-terminus contains the proteolytic domain of the serine protease type. The three dimensional structure of the holoprotein is currently unknown. However, the structures of all kringle domains as well as the proteolytic domain have been established. In the following, structural features of each domain are examined, followed by a brief analysis of studies pertaining to gross features of the holoprotein.

1.3.2 N-Terminal Peptide

The N-terminal peptide of plasminogen consists of approximately 80 residues. In HPgn, the N-terminal residue is a glutamic acid thus the designation Glu-Pgn. Its structure is currently unknown. However, based on sequence homolgy, it is believed to adopt a fold similar to hepatocyte growth factors (Donate et al. 1994).

Functionally, the NTP of Pgn acts to maintain the compact conformation of the zymogen. It does so by ligating to a subsequent domain thereby maintaining the compacted conformation. The exact site of such a ligation is not precisely known. There is evidence that Lys50 or Lys62 of the NTP interacts with kringle 5 through lysine binding sites (An et al. 1998;Cockell et al. 1998).

Ligation of the closed conformation of Pgn brings the NTP region into a close proximity with the proteolytic domain. Chemical cross-linkage studies suggest a model where kringle 2 is within contact of the protease domain in the closed conformation of

Pgn (Banyai, Patthy 1985). This favors the model whereby the NTP is ligated to a subsequent kringle domain.

Implications of this model extend beyond simple ligation of the closed conformation of unactivated Pgn. Taken together, evidence that the NTP ligates to kringle 5 would indeed place it within close proximity of the protease domain. Such proximity in the closed conformation possibly confers resistance towards unnecessary activation by shielding the activation bond from endogenous activators (Ponting et al. 1992).

1.3.3 Kringle Domains

Following the NTP of Pgn are five homologous domains individually referred to as kringles. Each kringle contains approximately 80 residues connected to adjacent kringles by linkers of various lengths. The linkers impart a degree of flexibility to the holoprotein. However, covalent inter-kringle contacts also exist which probably restrict this flexibility (Abad et al. 2002). Kringles are found in many proteins where they may be present at large numbers. Such is the case for lipoprotein(a). It contains a variable number of kringle domains often present at numbers greater than 20 (Fless et al. 2000).

The structures of all five kringle domains in HPgn have been determined. Figure 7 illustrates their overall similarities. Each kringle is folded into a compact unit containing four anti-parallel β-sheets connected by contorted loops. Within each kringle is an identical network of three disulfide bonds, a common motif observed in all such domains.

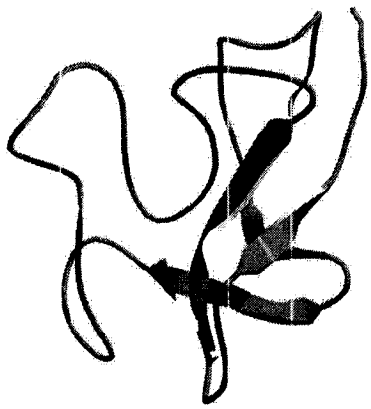

Kringle One Monomer
PDB ID: 1CEA

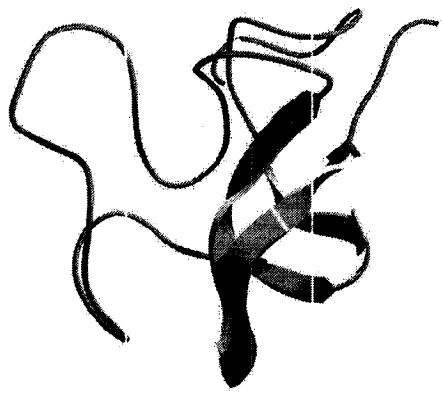

Kringle Two Monomer
PDB ID: 1B2I

Angiostatin Fragment
Kringles One - Three
PDB ID: 1KIO

Kringle Four Monomer
PDB ID: 1PK4

Kringle Five Monomer
PDB ID:5HPG

Figure 7: Kringle Domains of Plasminogen. Plasminogen contains five homologous kringle domains. The crystal structures of each domain are shown along with their respective PDB accession numbers (Abad et al. 2002;Chang et al. 1998;Marti et al. 1999;Mathews et al. 1996;Mulichak et al. 1991). Angiostatin (Center) is an internal fragment of plasminogen comprised of a variable number of kringles 1-4 (Abad et al. 2002).

1.3.3.1 Kringle Domains Contain Lysine Binding Sites

With the exception of kringle 3, each kringle contains binding sites for lysine and lysine analogs. The lysine binding sites (LBS) are responsible for maintaining the closed conformation of DPgn as well as binding to fibrin and other cellular surfaces. Contained within each LBS are similar determinants necessary for ligand binding. In particular, each binding site contains regions involved in stabilizing both the electrostatic and hydrophobic structural constituents present in lysine and lysine analogs. Figure 8 illustrates this concept.

Shown in Figure 8 is an enlarged view of the LBS of kringle 4. Bound is the lysine analog, 6-AH. The binding site is a pocket composed of a hydrophobic region flanked by charged extremities. Tryptophan residues at positions 62 and 72 (kringle 4 numbering) provide hydrophobic contacts which favorably interact with methylene groups present in 6-AH. Further stability is provided by charged groups at either end of the binding site. Negative charges are provided by Asp residues at positions 55 and 57 while positive charges are provided by Arg and Lys residues located at positions 71 and 35 respectively. While Figure 8 depicts 6-AH as the ligand bound, proteins possessing C-terminal lysine, i.e. fibrin, bind in the same fashion.

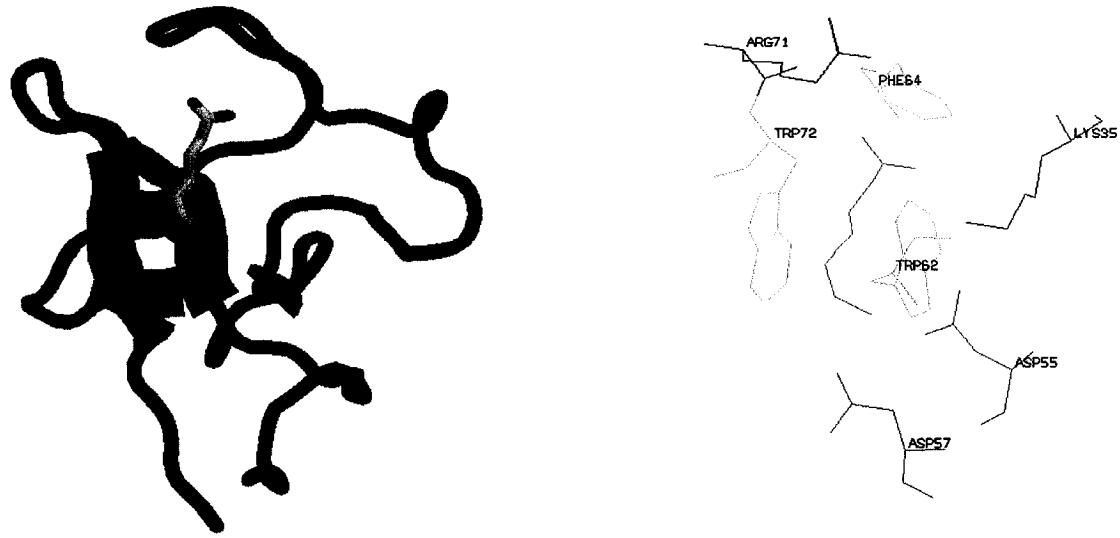

Figure 8: Kringle Domains Contain Lysine Binding Sites. Human plasminogen kringle 4 (PDB ID: 2PK4 (Wu et al. 1991)) is shown (Left) with a bound molecule of 6-aminohexanoate. An enlarged view of the lysine binding site (Right) showing residues involved in the binding of lysine and lysine analogs (PDB ID: 1PK4 (Mulichak et al. 1991))

Binding affinities for the LBS differ with respect to each kringle. They have been studied in both isolated kringles and in the holoprotein. In the holoprotein, binding at kringles 1 and 4 is the strongest while kringles 2 and 5 bind the weakest (Kornblatt 2000;Kornblatt et al. 2001). Kringle 3 does not bind lysine analogs as it does not possess a functional binding site.

1.3.3.2 Angiostatin: An Internal Fragment Containing Kringles 1-4

Illustrated in the center of Figure 7 is angiostatin, an internal fragment of Pgn comprised of kringles 1-4. As it has important clinical implications in its own right angiostatin will be briefly examined. Angiostatin is formed from proteolytic processing of plasminogen by metalloproteases including macrophage metalloelastase, as well as plasmin (Pirie-Shepherd et al. 2002).

Of clinical importance is the ability of angiostatin to inhibit angiogenesis, the proliferation of vascular endothelial cells (Ohyama et al. 2004). In doing so, angiostatin is believed to inhibit the recruitment of a vasculature network needed to support the growth of tumors. For the purpose of this study only the knowledge that angiostatin is comprised of an internal multi-kringle fragment of Pgn is necessary.

1.3.4 Protease Domain of Plasminogen

The proteolytic domain of Pgn is a typical serine protease characterized by the presence of a conserved Asp-His-Ser catalytic triad. In HPgn, the domain contains approximately 250 residues. Illustrated in Figure 9 is the three dimensional structure of the HPgn protease domain.

Figure 9: Crystal Structures of Human Plasminogen Proteolytic Domain. Left: Plasminogen proteolytic domain: The structure is rotated to display the residues comprising the catalytic triad. The residues are colored red. Clearly visible are the two subdomains. Right: Superposition of the alpha carbon traces of human plasminogen (red) and bovine trypsinogen (blue). The folds are nearly identical with a RMS deviation of 1.10 Å. PDB Accession numbers: plasminogen: 1RJX (Terzyan et al. 2004), trypsinogen: 1TGB (Fehlhammer et al. 1977;Peisach E. et al. 1999)

The tertiary structure of the protease domain is folded into two subdomains. Each subdomain is comprised of a β-barrel motif separated by loops. The representation illustrated in Figure 9 views down the axis of one barrel. The axis of the second barrel is parallel to the plane of the paper and is perpendicular to the first barrel.

There is considerable sequence homology between the Pgn protease domain and other serine proteases such as trypsin(ogen) and chymotrypsin(ogen). Both share approximately 40% sequence identity and approximately 50% similarity. Illustrated in Figure 9 is an alignment of the α-carbon backbone traces between Pgn and bovine trypsinogen. The overall folds are remarkably similar with a RMSD of 1.10 Å between the two backbones.

It is worthwhile to point out a feature shared between Pgn and chymotrypsin(ogen). Conserved between the two proteins is a disulfide. In HPgn, this disulfide bridges Cys548 and Cys666. In chymotrypsin(ogen), the similar disulfide is located between Cys1 and Cys122. For reasons that will become evident, this disulfide becomes relevant with regards to ligand binding properties shared between the two proteins.

1.4 Conformational Changes Observed in Plasminogen

The structure adopted by the Pgn holoprotein has been difficult to determine. This is likely due to the conformational flexibility inherent in its modular makeup. For example, the equilibrium constant for the opened/closed conformation of Pgn falls somewhere in the range of 0.05 to 0.2 (Markus G. 1996). Up to 20% of a population comprised of Glu-Pgn adopts the opened conformation at any given moment. This

conformational flexibility makes formation of crystals suitable to diffraction techniques difficult. Other techniques have been successfully applied to gain insights on the gross structural properties exhibited by Pgn in both the compact (closed) and extended (opened) conformations.

The gross shape adopted by the closed conformer of the Pgn holoprotein has been examined with electron microscopy (Tranqui L. et al. 1979). The results suggested that this conformation of Pgn adopts a compact structure, best characterized by the shape of a right handed spiral. In this model, the NTP partially overlaps the protease domain. This agrees with other studies where kringle 2 was shown to lie in close proximity to the protease domain (Banyai, Patthy 1985).

Microscopy has also been employed to examine the opened conformation of Pgn. Here the protein was shown to adopt a roughly U-shaped geometry resulting from expansion of the closed conformation (Wesiel J.W. et al. 1984). Thus, the protein adopts a more spherical shape in the closed conformation and a more extended shape in the opened conformation.

Perhaps the most rigorous evidence for this conformational change has been provided by application of analytical ultracentrifugation (AUC). The conformational transition induced upon the binding of lysine analogs is readily observed with the technique of AUC and has been well characterized. Changes in sedimentation coefficients reflect this and have often been used to characterize this property of Pgn (Markus G. 1996). The closed conformation of HPgn sediments with a value of $S_{20,w}$ around 5.7 while the opened conformation sediments with a value of $S_{20,w}$ of about 4.7.

The conformational transition is also reflected in measured frictional ratios (f/f_o). Frictional ratios measure a protein's frictional coefficient relative to the frictional coefficient of an unhydrated sphere similar in size. This provides information on the shape and hydration of a macromolecule as it sediments. Ratios of f/f_o approaching a value of 1.0 reflect the sedimentation of a spherical globular protein. Deviations from this value reflect more extended shapes approaching that of a rod. The closed conformation of HPgn sediments with a value of f/f_o around 1.4 while the opened conformation sediments with a value of f/f_o around 1.7 (Castellino et al. 1973).

Beyond sedimentation analysis, the conformational change of Pgn as it binds lysine analogs has been studied from many different angles. Techniques used to characterize the transition include fluorescence polarization, (Castellino et al. 1973;Sugawara et al. 1984) small angle neutron scattering, (Mangel et al. 1990) stopped-flow fluorescence, (Christensen, Molgaard 1991) high pressure absorption spectroscopy/electrophoresis (Kornblatt et al. 1999) and isothermal titration calorimetry (Kornblatt et al. 2001). Similar findings are observed in all such studies whereupon the conformational change from a compact, closed structure is easily monitored as it changes to a more extended and opened structure.

The importance of this conformational change is underscored by the many agents that modulate the activation and activity of Pgn. The outline above established the presence of the conformational change prior to Pgn activation. Physiologically, formation of Lys-Pgn is the manifestation of this conformational change. In Lys-Pgn the excised NTP no longer ligates to a LBS, causing the structure to open. The extended conformation then exposes the activation bond, facilitating a stimulation of activation

rates. The ability of biological agents such as C-terminal lysine or lysine analogs to manipulate the conformational equilibrium of Pgn, bestows upon them a means of regulation.

Inherent in this regulation is the intrinsic flexibility possessed by Pgn. This flexibility allows it to undergo the aforementioned conformational change. A modular makeup where the domains are joined by flexible linkers gives Pgn the ability to easily change its conformation. The flexibility of Pgn is the final topic of this introduction. Agents able to report on protein flexibility are useful as probes of protein structure. One such agent is the fluorescent dye, 8-anilino-1-naphthalene sulfonic acid (ANS). The focus now shifts to ANS with a special attention on its useful properties as a protein structural probe.

1.5 Useful Properties of ANS

ANS, (Figure 10) is a fluorescent molecule capable of reporting on local environment. It has long been known that it exhibits a large increase in fluorescence quantum yield upon introduction into a nonpolar medium. This is illustrated in Figure 11. The quantum yield of free ANS in water is only about 0.004 while in a less polar solvent it can be as high as 0.98 (Uversky et al. 1998). This property establishes ANS as a useful probe to report on local dielectric.

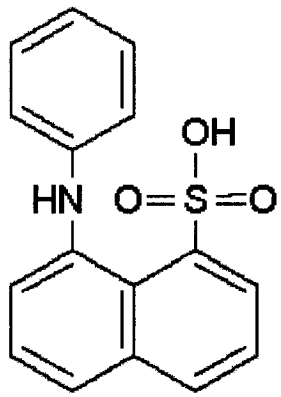

Figure 10: The fluorescent probe, 8-anilino-1-naphthalene sulfonic acid: Structural properties of many proteins have been assessed with information reported from ANS binding.

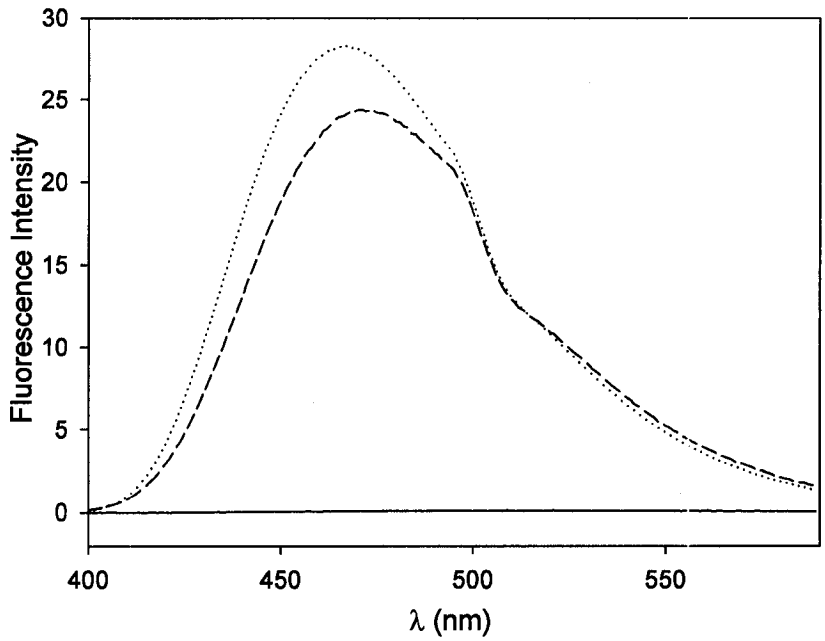

Figure 11: Fluorescence Emission of ANS: ANS undergoes a large increase in fluorescence quantum yield upon introduction into nonpolar solvents. The emission spectrum of ANS in water is negligible. (solid line) The emission of ANS (40 μM) bound to a protein such as BSA (2μM) (dashed line) mimics that of the probe in a less polar solvent (dotted line) as in isopropanol. Unless otherwise stated, ANS concentrations were 100 μM.

In a similar manner, ANS reports on local protein structure. Proteins that bind ANS often do so with similar fluorescent yields as observed for the dye in nonpolar solvents. This is illustrated in Figure 11. Upon binding to bovine serum albumin (BSA), ANS exhibits a similar fluorescence yield as does the free dye in a solvent of low polarity such as isopropanol. This is taken to mean that ANS reports on local hydrophobicity within the BSA structure.

BSA does in fact contain hydrophobic binding sites, as it functions to transport lipophilic substances throughout the bloodstream. In fact, the ANS-BSA system is a classic example of the use of ANS as a probe of local hydrophobicity. This system is perhaps the best characterized in the entire field of protein science and has paved the way for the many studies that followed (Weber, Daniel 1966).

1.5.1 A Brief History of ANS and Protein Science

Historically, ANS was first described by Stryer to report on local hydrophobicity. In this study ANS was shown to report on the solvent exposed hydrophobic pocket contained within apomyoglobin and apohemoglobin (Stryer L.S. 1965). Later, the pioneering work of Daniel and Weber led to an extensive analysis of ANS binding to BSA (Daniel, Weber 1966;Daniel, Yang 1973;Weber, Daniel 1966). These studies established a framework for the use of ANS as a probe of local hydrophobicity. They led to numerous studies involving the use of ANS as a probe for many different aspects of protein structure and function. A few of these will be examined.

1.5.2 ANS Probes Many Facets of Protein Structure and Function

Studies of ligand binding have often recruited the ability of ANS to report on binding sites of a hydrophobic nature. In such studies ANS competes for sites occupied by endogenous ligands. An example of this involves the RecA protein of *E. coli*, involved in the homologous recombination of DNA strands. ANS was found to bind at three sites within the protein (Masui, Kuramitsu 1998). Binding was diminished upon introduction of synthetic polynucleotides and ATP, suggesting that ANS bound to these sites.

Regions involved in molecular recognition have been located from information reported by ANS. The chaperonin GroEL has been characterized in this manner (Seale et al. 1995). GroEL is involved in, among other things, protein folding. A region thought to play an important role in molecular recognition was probed by photoincorporation of bis-ANS, a dimerized variant of ANS, into GroEL. The results obtained confirmed evidence from an earlier crystallographic study which implied the same region as being important in molecular recognition.

In another recognition study, protein-protein interactions between u-PA and its receptor (u-PAR) were probed with ANS. The u-PA receptor is an integral membrane protein containing a solvent exposed binding site for u-PA. ANS was shown to bind to a solvent exposed site on the surface of u-PAR (Ploug et al. 1994). Bound ANS was displaced upon addition of u-PA, fragments thereof, and anti-u-PA monoclonal antibodies. It was therefore concluded that ANS reported on the same binding surface implicated in binding u-PA.

1.5.3 ANS as a Probe of Protein Flexibility

Perhaps most relevant to the present study is the ability of ANS to probe protein flexibility. Many studies have recently focused on this characteristic of ANS. Protein flexibility is important in all aspects of biological function. There are many known examples of ligand binding occurring to a particular protein conformer induced by the ligand itself. ANS has been successfully used to probe such occurrences.

An elegant example of this was illustrated in a study of MurA, an enzyme responsible for bacterial cell wall synthesis. ANS was found to induce the formation of a binding site within a flexible loop known to be important during the catalytic cycle (Schonbrunn et al. 2000). This induced fit involved a major restructuring of the loop. It was suggested that a properly designed antibiotic would preferably sample the induced conformation and in doing so inhibit cell wall production. In this particular system, protein flexibility was required for maintenance of proper enzymatic function. However, in other systems, protein flexibility might not involve such maintenance. Such is true for the flexibility observed in molten globules.

1.5.3.1 Protein Flexibility and the Molten Globule

Flexibility is also a determinant in protein folding. The degrees of freedom exhibited by rotations about Φ and Ψ angles within the polypeptide backbone constitute this flexibility. For a protein to properly fold, it must possess a large degree of flexibility in order to sample enough populations along the folding pathway. In doing so, the native fold is predominantly maintained while similar, yet more energetic conformers temporally fluctuate around the global minimum.

Conditions stabilizing these higher energy conformers promote molten globule formation. In this respect, a molten globule retains the secondary structural characteristics of the native protein while possessing enough flexibility to sample alternative populations distinct from the native fold (Ptitsyn 1987). Often, these alternative conformers can be detected with ANS.

Presumably, a molten globule exposes to a larger degree, the hydrophobic core contained within its native fold. Conditions favoring this exposure also favor ANS binding, and as such are taken to be a fingerprint for the existence of a molten globule. Many proteins unfolding along the pathway of a molten globule have been detected with ANS. Examples include pectate lyase C, (Kamen, Woody 2001) carboxypeptidase Y, (Dumoulin M. et al. 1999) DnaK, (Shi et al. 1994) and α-lactalbumin (Bino J. et al. 2001).

1.5.4 Structural Evidence of ANS Binding

Despite the many studies having used ANS as a structural probe, very few crystal structures exist to substantiate the belief that ANS binds to predominately hydrophobic sites. Of the currently four available structures, three have positively identified hydrophobic binding sites (Ory, Banaszak 1999;Schonbrunn et al. 2000;Lartigue A. et al. 2003). The remaining structure shows ANS bound to chymotrypsin at a solvent exposed site with no hydrophobic determinants (Weber et al. 1979). Despite this singular discrepancy, the finding that ANS binds to chymotrypsin at all is relevant to the present study as it pertains to Pgn.

1.5.5 Plasminogen Conformational Flexibility and ANS

This introduction was designed to inform the reader on the importance of flexibility with regards to Pgn function. The ability of activators and effectors to modulate Pgn activation rates relies on the ability of Pgn to easily change its conformation. This is reflected in the intrinsic flexibility of Pgn, a function ultimately linked to its modular structure. Flexibility has been investigated in the past from information obtained upon characterization of protein-ANS binding interactions. Many of the investigations were rewarded with structural information relevant to the biological function of the system examined. This project investigates the flexibility of the canine variant of Pgn, (DPgn) through information reported upon ANS binding.

It is worthwhile to point out that while this study utilizes the canine variant of Pgn, it likely reflects similar properties of the human variant. At the onset of the study, a clone of HPgn was not immediately available. It was a trivial matter to obtain dog blood from which DPgn was easily prepared. The canine variant is similar to the human variant. Within the known regions of its entire sequence, (10% is unknown to date) DPgn shares 88% sequence identity (Schaller et al. 1989) and is similar with respect to activation rates catalyzed by u-PA and streptokinase (Schaller, Rickli 1988;Wohl et al. 1983). It is therefore reasonable to assume that differences between DPgn and HPgn are marginal and information obtained from studies involving HPgn, are likely to reflect DPgn.

2.0 Materials and Methods

2.1 Reagents

All reagents were of analytical grade and used without further purification. Buffer constituents were from Fisher. ANS, ammonium salt was from Fluka. Porcine pancreatic elastase was from Sigma.

2.2 Plasminogen

Canine plasminogen was prepared from frozen plasma as described previously (Kornblatt et al. 2001). Approximately 1 liter of plasma was passed over a lysine-Sepharose affinity column containing around 12 mL of resin. Prior to loading, the column was equilibrated in a running buffer consisting of 0.1 M Potassium Phosphate, 1 mM EDTA and 0.3 μM aprotinin (bovine trypsin inhibitor), pH 7.5. The column was washed until the flowthrough OD_{280} equaled that of the running buffer. Bound DPgn was eluted with a minimal volume of elution buffer whose composition contained equal concentrations of all running buffer constituents plus 5 mM 6-AH.

Eluted DPgn was then dialyzed exhaustively against 5 mM Tris-HCl, 5 mM EDTA and 50 mM NaCl to remove virtually all bound 6-AH. This was necessary since in DPgn, kringle four binds 6-AH with a K_d of about 7 μM (Kornblatt et al. 2001). Upon completion of dialysis, the calculated concentration of 6-AH was less than 1 nM whereupon the DPgn was separated into mg quantities and lyophilized overnight. Lyophilized product was then sealed under vacuum and stored at -20 °C until needed. This method took approximately 3 days until completion and yielded one band on an overloaded 7% SDS-PAGE gel. Typical protein yields were on the order of 40 mg DPgn per liter of plasma.

2.3 Determination of Sample Concentrations

Plasminogen concentrations were determined spectrophotometrically using an $\varepsilon^{0.1\%}$ of 1.5 at 280 nm and a value of 90,100 Da for the molecular weight (Kornblatt et al. 1999). ANS concentrations were calculated from the absorbance at 360 nm using an ε ($M^{-1}cm^{-1}$) of 5800, determined spectrophotometrically. Concentrations of all species were determined on a Cary 100 UV-VIS spectrophotometer thermostated at 15 °C.

2.4 Demonstration of ANS Binding

Native electrophoresis was conducted in a BioRad Mini-Protean III electrophoresis system. Polyacrylamide gels were prepared (7 %T, 2.67 %C) and predeveloped in buffer by applying a voltage across the gel (90 V) until the current load no longer changed. At this point, the running buffer (80 mM β-Ala and 40 mM acetic acid, pH 4.4) was changed and the protein samples loaded.

Protein was loaded at 5 - 20 μg per lane and developed at 90 V for three hours. Developed gels were then washed and equilibrated for 20 minutes in a citric acid – phosphate equilibration buffer (79 mM citric acid, 41 mM sodium phosphate dibasic and 0.1 M NaCl, pH 3.0). Gels were then stained for 20 minutes in a staining buffer identical to the equilibration buffer plus 1 mM ANS. Bound ANS was visualized on a UV transilluminator and photographed using a Bio Doc-It™ documentation system from UVP. After documentation, gels were Coomassie Blue stained.

2.5 Fluorescent Titrations of DPgn with ANS

DPgn (10 μM) was prepared by reconstituting 5 mg of lyophilized product into the appropriate buffer and dialyzing overnight at 4 °C against approximately 200 volumes of buffer. Aprotinin was included (0.3 μM) to prevent conversion to plasmin. Titrations utilized the following buffer systems: 79 mM citric acid, 41 mM sodium phosphate dibasic, pH 3.0; 80 mM β-Alanine, 40 mM acetic acid, pH 4.5; 0.1 M sodium phosphate dibasic, 0.1 M NaCl, pH 6.5.

Titrations were conducted on an Aminco-Bowman AB2 luminescence spectrometer thermostated at 15 °C. The fluorimeter was equipped with a magnetic stirrer. ANS was added with a micropipettor set for 2 μl increments. After each addition, the system was equilibrated by stirring for 2 minutes prior to recording spectra. The total volume was 2 ml at the start of an experiment and contained in a 3 ml cuvette of pathlength 1.0 cm. Fluorescence enhancement at 470 nm was used as the signal indicative of ANS bound to DPgn. Instrumental settings utilized an excitation slit width (λ_{ex} = 350nm) of 4 nm and emission slit width of 4 nm.

Photomultiplier voltages were set such that the observed fluorescent yield was within 80% of maximum intensity for each experiment. Resulting binding isotherms were then normalized to facilitate direct comparison between the different experimental conditions. To this end, all binding data were normalized to a standard of 0.1 μM quinine sulfate in 0.1 M H_2SO_4.

The titration protocol covered a molar ratio (ANS/DPgn) from 0 to 5. Beyond 100 μM ANS, corrections due to inner-filter effects exceed a factor of two. Titrations were

not carried out beyond 60 μM ANS. Inner-filter effects present below 60 μM ANS were corrected with the equation,

$$F_c = F_o \times \text{antilog}\left(\frac{OD_{ex} + OD_{em}}{2}\right) \qquad \text{Equation (1)}$$

where F_c and F_o refer to the corrected and observed fluorescence respectively, OD_{ex} refers to absorbance at the excitation wavelength (350 nm) and OD_{em} refers to the absorbance at the emission wavelength (470 nm). Such corrections did not exceed a factor greater than 1.4. Corrections were also applied to account for changes in volume due to dilution of DPgn. These corrections were not greater than 5%. Finally, a blank titration of ANS into buffer was subtracted from the experimental data set to correct for the fluorescence of free ANS.

ANS binding isotherms were generated by plotting the corrected fluorescence intensity at 470 nm as a function of ANS concentration. Plots were then analyzed with SigmaPlot. Saturation was not evident at the concentrations chosen for the experiments. For this reason, plots were not fit to equations describing binding and were used rather, to qualitatively assess the effect of pH upon ANS binding.

2.6 Fluorescence Enhancement of ANS as a Function of pH

The effect of pH within the range of 3.0 to 6.0 on the fluorescence enhancement of bound ANS at a constant molar ratio of ANS/DPgn was examined. This allowed for the determination of the pH optimum for ANS binding. Subsequent characterization would then focus primarily on conditions favoring enhanced binding.

Protein samples were prepared as follows. Samples containing DPgn (11 μM) were dialyzed separately with ANS containing (60 μM) buffers whose pH fell within the range specified above. Aprotinin (0.3 μM) was added to each sample in order to minimize conversion to plasmin. Samples were dialyzed overnight in the dark so as to minimize photodegradation of ANS. The experimental buffer systems are described in Table 1.

[citric acid]	[Sodium Phosphate Dibasic]	[NaCl]	[ANS]	pH	Calculated Ionic Strength (M)
79.5 mM	41.1 mM	0.1 M	60.0 μM	3.0	0.35
71.5 mM	57.0 mM	0.1 M	60.0 μM	3.4	0.42
61.5 mM	77.1 mM	0.1 M	60.0 μM	4.0	0.51
55.9 mM	88.2 mM	0.1 M	60.0 μM	4.3	0.56
48.5 mM	103.0 mM	0.1 M	60.0 μM	5.0	0.65
44.3 mM	111.5 mM	0.1 M	60.0 μM	5.3	0.70
36.9 mM	126.3 mM	0.1 M	60.0 μM	5.9	0.78

Table 1: Experimental conditions used to examine the effect of pH upon ANS binding at a constant molar ratio of ANS/DPgn.

Fluorescence emission spectra were collected utilizing similar parameters as discussed in the previous section with the exception of a photomultiplier voltage set at 575 V for all spectra recorded. Collected spectra were then corrected for the fluorescence of free ANS as well as inner-filter effects. Inner-filter corrections were made from direct absorbance measurements of the dialyzed samples upon completion of fluorescence measurements. Finally, the corrected values of fluorescence at 470 nm were plotted as a function of pH.

2.7 Fluorescence of Free ANS

The fluorescence of free ANS was examined as a function of pH. Dialysis buffers containing ANS provided a means to assess the contribution of free ANS towards the signal observed in the presence of DPgn. Spectra of free ANS were determined by subtraction of dialysis buffers void of ANS. These spectra were recorded in an identical manner as previously described.

2.8 Calculation of Buffer Ionic Strength

The ionic strengths of buffers utilized in the fluorescence experiments were calculated using equation 1 below,

$$1/2 \sum_i c_i z_i^2 \qquad \text{Equation (2)}$$

where z is the charge of each species i, and c is its concentration. The charges and concentrations of each ionic species were in turn approximated from calculations utilizing the Henderson-Hasslebach equation.

2.9 Determination of ANS Binding Affinity: Isothermal Titration Calorimetry

Isothermal titration calorimetry (ITC) was used to determine the binding constants of ANS to DPgn. The method is sensitive and reproducible and bypasses many of the complications in data analysis arising from the use of steady-state fluorescence.

DPgn (40 μM) was prepared by reconstitution of lyophilized product into an appropriate buffer to a total volume of 2.5 ml. This was dialyzed overnight against a 200-

fold excess of buffer at 4 °C. Aprotinin was added (0.3 μM) to the sample both prior to and after dialysis to minimize conversion to plasmin.

Buffers were chosen to control both the conformation of DPgn (closed vs. opened) and pH. Buffer compositions were as follows: 1. *closed, low pH:* 79 mM citric acid, 41 mM sodium phosphate dibasic, 0.1 M NaCl (pH 3.0) 2. *opened, low pH:* 79 mM citric acid, 41 mM sodium phosphate dibasic, 0.1M NaCl, 50 mM 6-AH (pH 3.0) 3. *closed, neutral pH:* 30 mM citric acid, 140 mM sodium phosphate dibasic, 0.1M NaCl (pH 6.4) 4. *opened, neutral pH:* 30 mM citric acid, 140 mM sodium phosphate dibasic, 0.1M NaCl, 50 mM 6-AH (pH 6.4).

After overnight dialysis, DPgn samples were centrifuged for 30 minutes at 14 kRPM to remove particulates. Particulates were also removed from the dialysis buffers by filtration through Whatman 1 filters. Filtered buffers were then used to prepare the ANS solutions employed in subsequent titration experiments.

Titrations were conducted on a Microcal VP-ITC. All experiments were thermostated at 15 °C in a cell volume of approximately 1.5 ml. ANS (1 mM) was added over 37 injections of 7 μl each to cover a molar ratio (ANS/DPgn) from 0 to 5. Instrumental parameters utilized a reference power of 0 μcal/sec and a stirring speed of 300 RPM. Blank titrations of ANS into buffer were subsequently determined and subtracted from DPgn containing samples to remove thermal contributions of ANS dilution.

Data was analyzed using the Origin analysis package provided with the VP-ITC instrument (MicroCal™ Inc. 1998). Binding isotherms were generated from integrated raw heat changes associated with the addition of ANS into the sample cell. Resulting

isotherms were then fit to a ligand binding model involving three independent binding sites. Attempts to fit the data to models containing one or two independent sites yielded poor fits and were not considered further. Having chosen an appropriate model, the data were subjected to a Marquardt minimization routine. Typically, the data converged to a minimized chi-squared value after three rounds of ten iterations. Residuals were randomly distributed indicating a reasonable fit.

2.10 The Dependence of DPgn Flexibility upon pH: Analytical Ultracentrifugation

Analytical ultracentrifugation (AUC) sedimentation velocity experiments were employed to assess the effect of pH upon DPgn flexibility. DPgn samples (7 μM) were prepared by reconstitution of lyophilized product into an appropriate buffer to a total volume of 1 ml. Samples were then dialyzed overnight against the respective experimental buffers at 4 °C. Aprotinin was added to 0.3 μM both before and after dialysis to minimize conversion to plasmin. Buffers were identical to those listed above for the ITC experiments.

A Beckman XLI analytical ultracentrifuge was used to determine the sedimentation velocity profiles of DPgn. Experiments were conducted at 15 °C and a rotor speed of 37 kRPM. Samples were equilibrated overnight under vacuum in the centrifuge rotor to ensure thermal equilibrium. Sedimentation patterns were followed at 280 nm using absorption optics.

Sedimentation velocity analyses were determined with the program SedFit (Schuck 1998). A continuous c(s) model was employed to determine observed sedimentation coefficients (s^*) from sedimentation velocity profiles. Apparent values of

s^* were determined by the program from simulations of the Lamm equation describing macromolecular mass transport. In addition to s^*, the frictional ratios and sample meniscus positioning were fit, while the bottom of the sample cell was not. Upon completion of modeling all generated fits contained RMSD values of 0.025 or less. The residuals obtained from modeling were randomly distributed and indicated reasonable fits to the experimentally observed data.

Calculated s^* values were transformed to $S_{20,w}$ values to reflect the s value of each species in water at 20 °C using the equation,

$$S_{20,w} = S^* \left(\frac{\eta_{T,B}}{\eta_{20,w}} \right) \frac{(1 - \bar{\upsilon}\rho)_{20,w}}{(1 - \bar{\upsilon}\rho)_{T,B}} \qquad \text{Equation (3)}$$

where η and ρ refer to the viscosity and density at the respective experimental temperature (T) of buffer (B) while the subscript 20,w refers to identical values of water. The partial specific volume of DPgn at the respective temperature is designated υ-bar. Values representing the experimental conditions were determined as described below.

Buffer densities and viscosities at the experimental temperature were calculated with the program Sednterp (http://www.rasmb.bbri.org/). Buffers containing 6-AH, were approximated with creatinine, a structural analog. Both are zwitterionic in character and similar in size. The calculated densities and viscosities used in subsequent analyses are listed in Table 2 below.

Buffer	pH	ρ (g/ml) at 15 °C	η (P) at 15 °C
Closed	6.3	1.02478	0.012595
Opened	6.3	1.02562	0.012655
Closed	3.0	1.01523	0.012146
Opened	3.0	1.01696	0.012244

Table 2: Hydrodynamic Parameters Used to Determine DPgn Sedimentation Characteristics. Tabulated are the calculated values used in the sedimentation modeling of DPgn. Values were calculated from known buffer compositions (see text) using the program Sednterp.

Also required for the AUC data analysis is the partial specific volume (v-bar) of DPgn. The value of 0.7165 ml/g at 15 °C was calculated from the primary sequence of DPgn, again using Sednterp. The complete primary sequence of DPgn is unknown. A chimeric sequence was constructed, using known sequenced regions of DPgn including the NTP, K1-K3, and miniplasminogen (Pirie-Shepherd et al. 2002;Schaller, Rickli 1988;Schaller et al. 1989). This sequence was aligned with the known sequence of HPgn. Regions within the DPgn sequence not determined to date were replaced with homologous regions from the HPgn sequence. In all, 63 unknown residues from DPgn were accounted for from the HPgn sequence in both the NTP-K1 and K4 regions. The constructed sequence is illustrated in Figure 12.

```
  1 SLLDDYVNTQ GASVFSLTKK QLSVGSIEEC AAKCEEDEEF TCRAFQYHSK EQQCVIMAEN
 61 RKSSIIIRMR DVVLFEKKIY LSECKTGNGK TYRGTMAKTK NDVACQKWSD NSPHKPNYTP
121 EKHPLEGLEE NYCRNPDNDE NGPWCYTTNP DVRFDYCNIP ECEEECMHCS GENYEGKISK
181 TKSGLECQAW NSQTPHAHGY IPSKFPSKNL KMNYCRNPDG EPRPWCFTMD PNKRWEFCDI
241 PRCTTPPPPS GPTYQCLKGR GESYRGKVSV TVSGHTCQHW SEQTPHKHNR TPENFPCKNL
301 DENYCRNPDG ETAPWCYTTN SEVRWEHCQI PSCESSPITT EYLDAPASVP PEQTPVVQEC
361 YHGNGQSYRG TSSTTITGRK CQSWSSMTPH RHEKTPEHFP EAGLTMNYCR NPDADKSPWC
421 YTTDPSVRWE FCNLRKCSGT EASVVAPPPV VLLPDVETPS ASDCMFGNGK GYRGKKATTV
481 MGIPCQEWAA QEPHRHSIFT PETNPQAGLE KNYCRNPDGD VNGPWCYTMN QRKLFDYCDV
541 PQCVSTSFDC GKPQVEPKKC PGRVVGGCVA NPHSWPWQIS LRTRYGKHFC GGTLISPEWV
601 LTAAHCLERS SRPASYKVIL GAHKEVNLES DVQEIEVYKL FLEPTRADIA LLKLSSPAVI
661 TSKVIPACLP PPNYVVADRT LCYITGWGET QGTYGAGLLK EAQLPVIENK VCNRYEYLNG
721 RVKSTELCAG NLAGGTDSCQ GDSGGPLVCF EKDKYILQGV TSWGLGCARP NKPGVYVRVS
781 RFVTWIEGIM RNN
```

Figure 12: The Primary Sequence of a DPGN/HPgn Chimera. Known sequences from the DPgn NTP, kringles 1-4 and the proteolytic domain were aligned with the known sequence of the HPgn holoprotein. Unknown regions contained within the DPgn sequence were substituted with homologous regions of the HPgn sequence. The substitutions are underlined. They account for less than 10% of the entire sequence.

DPgn flexibility was examined from modeled frictional ratios (f/f_o). The values of f/f_o give a measure of the hydration state and shape of a protein as it sediments in solution (Lebowitz et al. 2002). Frictional ratios were compared to determine the effect of pH upon the flexibility of DPgn in both its closed and opened conformations. They were determined during the refinements of initial s^* values in the SedFit fitting routines from modeled diffusion coefficients of each sedimenting species. Diffusion coefficients were, in turn, based upon boundary modeling analysis (Dam, Schuck 2004) of the sedimentation patterns incorporated into the SedFit fitting routines.

2.11 Conformational Change of DPgn and pH: Circular Dichroism

Near-UV circular dichroism spectroscopy (CD) was used to examine the effect of pH upon DPgn tertiary structure. DPgn (12 μM) was prepared by reconstitution of lyophilized product into a total volume of 1 ml using each respective experimental buffer. Samples were dialyzed overnight at 4 °C against 500 volumes of buffer. Aprotinin (0.3

μM) was added prior to dialysis to prevent conversion to plasmin. Buffer compositions were identical those listed for the ITC experiments.

A Jasco J-710 CD spectropolarimeter was used to examine DPgn tertiary structure. All spectra were taken at 25 °C in a 0.5 cm pathlength rectangular cuvette. The sample compartment was continually purged with nitrogen at a flow rate of 5 L min^{-1} to minimize spectral noise due to oxygen presence. Spectra were recorded from 240 – 320 nm at a scan rate of 20 nm min^{-1} at a bandwidth of 1 nm. Final spectra are reported as the average of five accumulations.

2.12 Localization of ANS Binding Sites: Native Electrophoresis

DPgn was proteolytically cleaved and the resulting fragments purified. Purified fragments were separated using native electrophoresis and stained with ANS to localize the binding sites and to determine the minimum number of binding sites distinguishable.

The method of Schaller (Schaller et al. 1985) was utilized to digest DPgn. DPgn (17 mg/ml) was prepared by reconstitution of lyophilized product to a total volume of 300 μl into a buffer containing 0.2 M Tris-HCl, pH 8.8. To this sample, porcine pancreatic elastase was added to a final enzyme:substrate ratio of 1:100 (w/w). Proteolysis was carried to completion overnight at 22 °C. A control reaction containing 50 μg DPgn alone was incubated overnight in the same manner. Similarly, a control containing elastase alone was incubated overnight.

Dialysis was performed the following day for three hours on the digested sample into a buffer containing 0.1 M Tris-HCl and 0.1M NaCl, pH 8.8. This was necessary to reduce the ionic strength of the sample. Elastase was supplied as a suspension in

saturated ammonium sulphate which interfered with the desired resolution of subsequent native electrophoresis steps.

The dialyzed sample was purified by application to a small amount of lysine-Sepharose (approximately 500 µl bed volume) packed into a Pasteur pipet. The column was equilibrated with a small amount of wash buffer containing 0.1 M Tris-HCl and 0.1M NaCl, pH 8.8. Proteolysis fragments void of lysine binding sites washed through the column while fragments containing such binding sites remained bound.

Washed fragments were set aside and bound fragments eluted with 1.5 ml of elution buffer containing 0.1 M Tris-HCl, 0.1M NaCl and 5 mM 6-AH, pH 8.8. Fractions of approximately 300 µl were collected. The fraction containing the highest OD_{280} was chosen for subsequent analysis. Concentrations of the purified fragments were determined spectrophotometrically by use of the Bradford assay.

Purified products were separated on a 10% native polyacrylamide gel in a manner identical to that described in Section 2.4 for the determination of ANS binding. After electrophoresis, gels were washed and equilibrated in buffer whose composition was also described above. Following equilibration, gels were stained for 20 minutes in ANS staining buffer. The gels were then placed on a UV transilluminator and documented. Finally, ANS stained gels were transferred to and stained overnight in Coomassie Blue to confirm the coincidence of protein containing bands with that of the ANS stained bands.

2.13 Preliminary Identification of Elastase Digested Fragments

Purified proteolytic products were separated in denaturing polyacrylamide gels to compare the fragmentation patterns of DPgn with the known elastase digest fragments of

HPgn. Identification of these fragments aided in the subsequent identification of bands observed in the native gels.

Purified fragments were separated on 10% SDS-PAGE gels at 100V. Gels were developed under both reducing and non-reducing conditions for comparison. This was necessary due to the fact that DPgn contains a complex network of disulfide bridges. Molecular weights of each fragment were estimated through measured R_f values. The measured values were then plotted against the log molecular weights of known standards. Molecular weights of DPgn fragments were then estimated from a linear fit to the standard curve.

3.0 Results

3.1 Plasminogen Binds ANS:

Binding of ANS was apparent from native PAGE experiments. Figure 13 shows the results of a typical experiment. The top panel depicts a gel stained in ANS. The resulting fluorescent patterns are observed upon UV transillumination. These patterns are easily distinguished over the background fluorescence. Furthermore, the same bands exhibiting ANS fluorescence stained with coomassie blue (middle panel). Taken together, this means that under favorable conditions DPgn binds ANS.

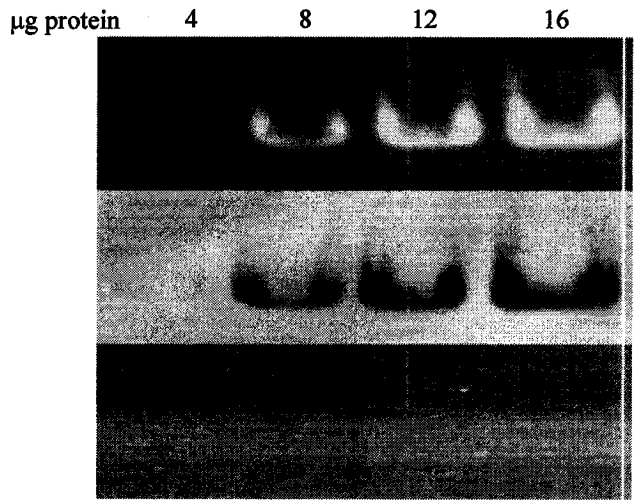

Figure 13: Canine plasminogen binds ANS. Results from native PAGE are shown. Top: 7% gel containing the indicated amounts of DPgn. After electrophoresis, the gel was equilibrated in buffer and subsequently stained with 1 mM ANS at pH 3.0. Middle: After documentation, the ANS stained gel was transferred to and stained in Coomassie Blue. Bottom: ANS binding is not detected at pH 6.3.

ANS binding was not observed at neutral pH. Figure 13 (bottom panel) shows a similar native PAGE experiment stained with ANS at pH 6.4. The gels were developed under identical conditions. However, at this pH one does not observe the fluorescent

bands noted at pH 3.0. Identical protein patterns were obtained when stained with Coomassie Blue indicating that DPgn binds ANS preferably at low pH.

3.2 Fluorescence Titrations Indicate Multiplicity of Binding Sites

Steady-state fluorescence was used to quantify the fluorescence emissions observed upon ANS binding. Figure 14 shows the emission spectra obtained. The observed spectra resemble that of ANS in nonpolar solvents or when bound to BSA, (Figure 11) indicating once again that DPgn binds ANS under favorable conditions.

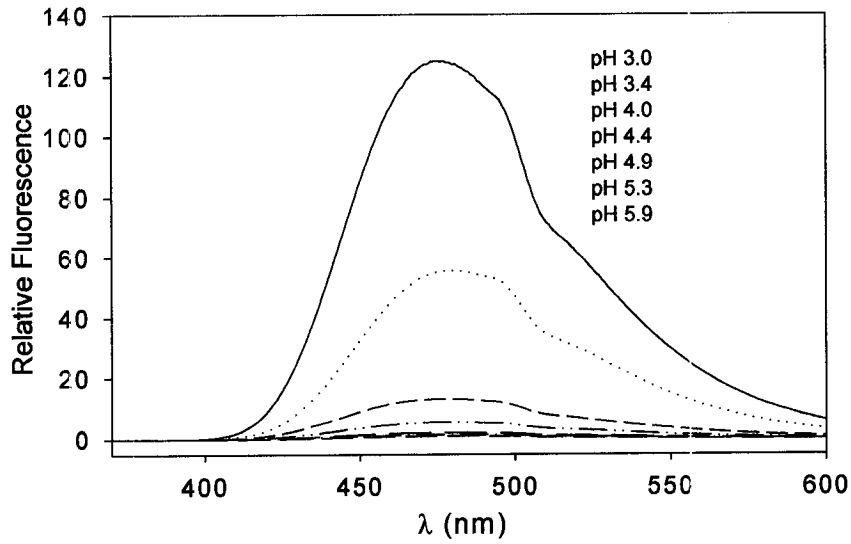

Figure 14: Fluorescence Emissions of ANS Bound to DPgn. DPgn (11 μM) was incubated with ANS (60 μM) and excited at 350 nm. The top spectrum reflects the system at pH 3.0. Subsequent spectra reflect the system at increasing pH values as indicated. The bottom spectrum reflects the system at pH 5.9.

When fluorescence intensity at 470 nm is plotted as a function of ANS concentration, the binding curves of Figure 15 are obtained. Here again, a pH dependence is noted where binding is favored at low pH. Fluorescent yields of ANS bound at low pH are dramatically enhanced compared to identical assay conditions at neutral pH.

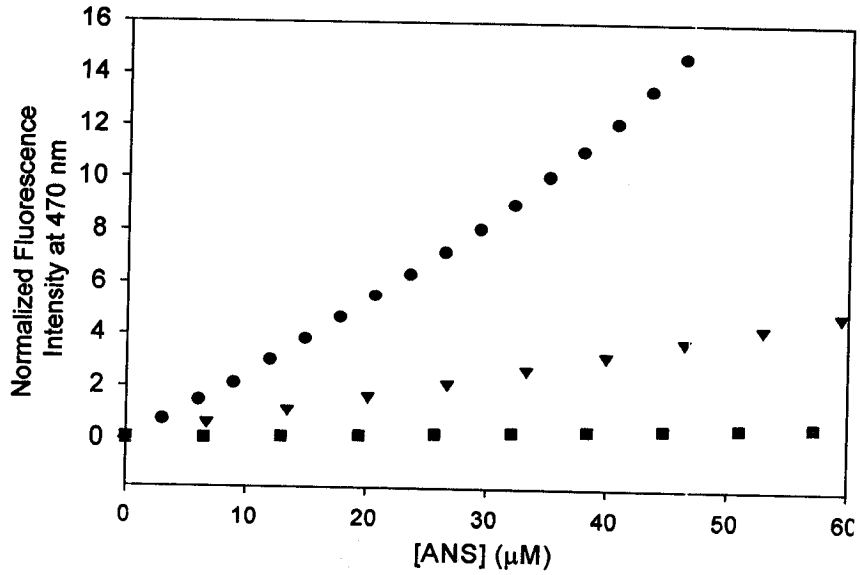

Figure 15: Fluorescence Titrations of DPgn with ANS. Illustrated are binding curves generated from titrations of 10 μM DPgn with the indicated amounts of ANS. Spectra were collected at 15 °C and normalized to a solution of quinine in H_2SO_4. The experiment was repeated at three different pH values: pH 3.0 (circles), pH 4.5 (triangles) and pH 6.5 (squares). Experimental data points are reported as the average of two independent experiments. While not reported, the errors associated with these averages did not exceed 2%.

The binding curves in Figure 15 are not indicative of simple binding. First, the plots do not reach saturation by 60 μM ANS. This is true regardless of the experimental pH and suggests that interactions between DPgn and ANS are weak. Regardless, the fact that binding is pronounced at lower pH suggests that the observed fluorescence enhancement is not due simply to non-specific binding. Since saturation is not evident under the conditions examined, binding cannot be described in simple terms defined by the equations of a rectangular hyperbola.

Despite the lack of saturation noted in the binding curves, information pertaining to binding can still be inferred. Careful examination of Figure 15 suggests that binding of ANS to DPgn is bimodal. This is especially true at low pH, where the curve is not linear. Rather, two regions exist with differing responses. At low concentrations of ANS there

exists a response, likely due to a binding site with low fluorescent yield. This trend continues up to concentrations of ANS near 20 μM. Beyond this region, a second mode of binding is observed. In this region, saturation is still not evident and is characterized by a binding site (or sites) with greater fluorescent yield. Taken together, this is interpreted to mean that DPgn contains multiple binding sites for ANS.

The presence of two or more ANS binding sites is adopted for the remainder of this thesis. This assumes the existence of a tight site with high affinity towards ANS, but low fluorescence quantum yield. This site corresponds to the first mode of binding noted in Figure 15 up to concentrations of ANS around 20 μM. Beyond this concentration, the remaining binding site(s) begins to fill. The remaining site(s) has weak affinity towards ANS, but a greater fluorescence quantum yield. This site corresponds to the second mode of ANS binding as noted in Figure 15 beyond 20 μM ANS.

3.3 ANS Binding is Enhanced at low pH

The steady-state fluorescence of ANS bound to DPgn was examined as a function of pH in order to assess its effect on binding. The results of such experiments are shown in Figure 16. As can be seen from this figure, ANS binds strongest at values approaching pH 3.0. Between pH 6.0 and 4.0, the fluorescence changes very little. However, the fluorescence intensity at pH 3.0 is approximately 120 times greater than that observed between pH 6.0 and 5.0. Between pH 4.0 and 3.0, the fluorescent yield increases approximately 6-fold.

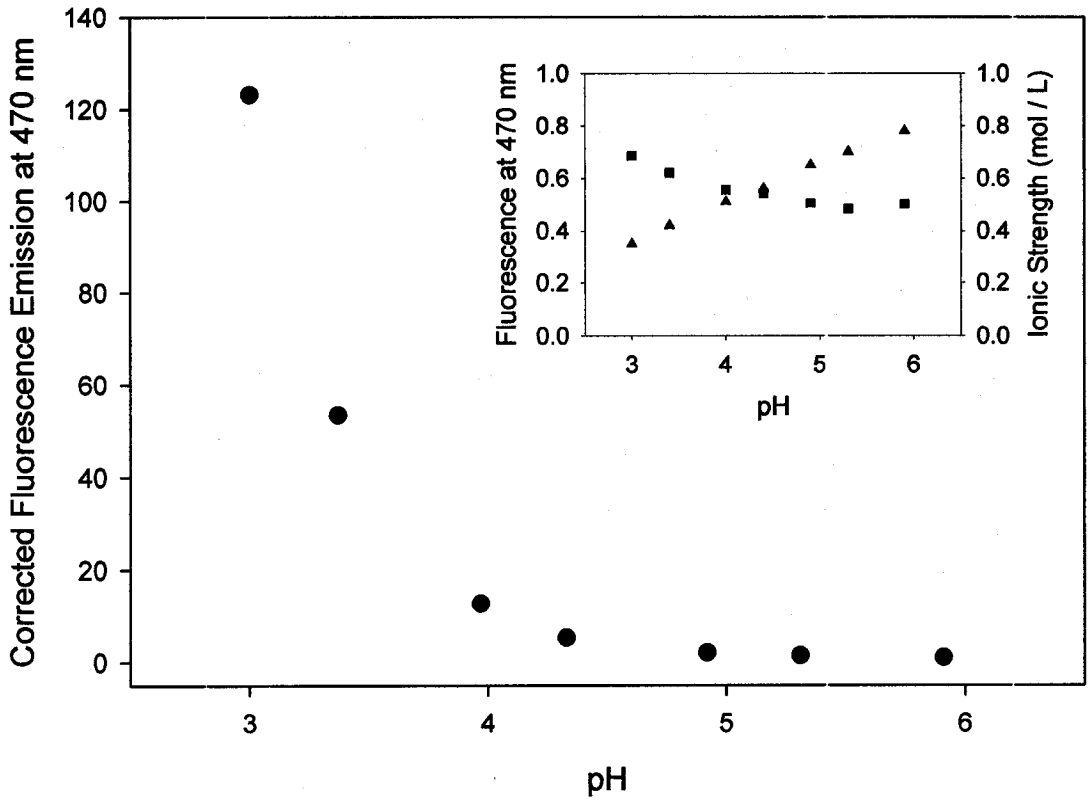

Figure 16: Binding of ANS is favored at low pH. DPgn (11 μM) was mixed with 60 μM ANS at the various pH values indicated. The fluorescence at 470 nm was determined from the resulting spectra of ANS bound to DPgn (circles). Inset: Fluorescence of free ANS (squares) as a function of pH. The scale matches that of DPgn containing samples. Also plotted are the calculated ionic strengths (triangles) of fluorescence buffers as a function of pH.

It is worthwhile to illustrate the nature of the buffers used throughout the course of the fluorescence experiments. In the aforementioned experiments, pH was varied at a constant molar ratio (ANS/DPgn) to assess its effect on binding. In this assessment, bound ANS was observed from an increase in the magnitude of fluorescence emissions at 470 nm. However, free ANS also exhibits an increased fluorescence yield at low pH. This is illustrated in Figure 16 (inset). This contribution towards the overall fluorescence in the presence of DPgn is small. While free ANS exhibits a higher fluorescent yield at low pH, it is marginal compared to the much greater fluorescent yield exhibited upon

binding to DPgn. As such, the enhanced fluorescent yield of ANS bound to DPgn at low pH is not due to a higher degree of ANS protonation.

The effect of ionic strength on binding interactions was examined. Table 1 lists the calculated ionic strengths of the buffers employed during the fluorescence experiments. It is important to note that the ionic strengths of the citric acid-phosphate buffer system increase with pH. The ionic strengths more than double upon increasing from pH 3.0 to 6.0. Concomitant with this increase is a decrease in the fluorescent yield of ANS, whether free or bound (Figure 16, inset). However, it is difficult to assess the cumulative effect, if any, these trends have on binding.

3.4 ANS Binding Constants Determined With Isothermal Titration Calorimetry

ITC was used to determine the binding constants of ANS towards DPgn. The method is reproducible, accurate and bypasses many of the complications arising from fluorescence techniques. Figures 17 through 20 show the results of ITC experiments.

Experiments were set up to examine binding of ANS as a function of pH as well as DPgn conformation. The binding of ANS to DPgn in the closed, compact conformation at low pH will be examined first. As seen in Figure 17, (top panel) the observed thermogram is exothermic and characterized by negative deflections from baseline upon subsequent injections of ANS. The measured heats initially decline until reaching a molar ratio (ANS/DPgn) approaching 1.0. Beyond this molar ratio the heats increase steadily and show no signs of saturation upon reaching a six-fold molar excess of ANS.

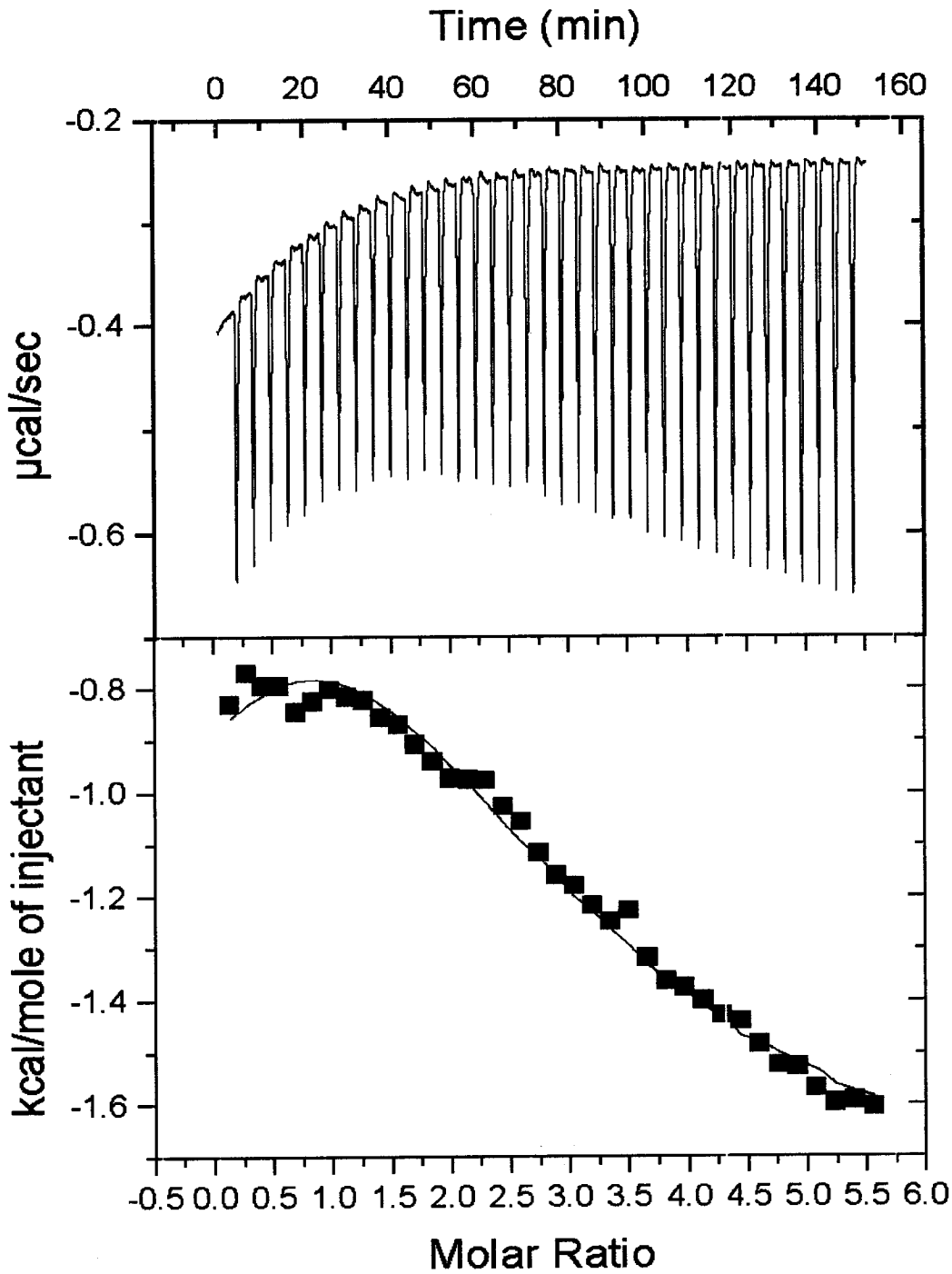

Figure 17: ITC Determination of ANS Binding Constants in the Closed Conformation of DPgn at pH 3.0. DPgn (40 µM) was titrated with 1 mM ANS over the molar ratios indicated. Top: Observed heats measured upon injection of ANS. Bottom: ANS binding isotherm resulting from integration of spikes observed during the titration. The isotherm was fit to a model involving three independent binding sites for ANS. Squares represent experimental data points while the line indicates the best fit to the experimental data.

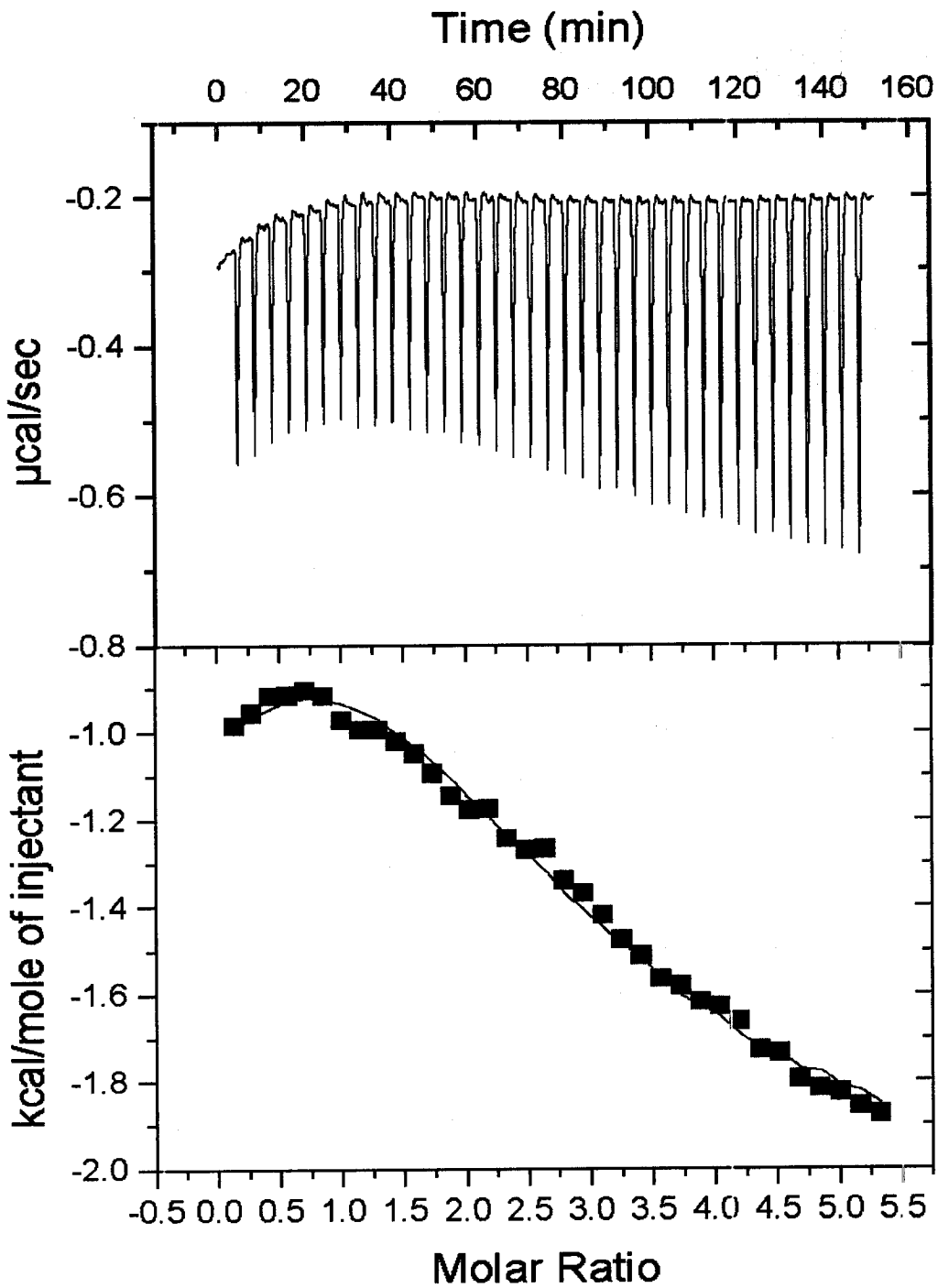

Figure 18: ITC Determination of ANS Binding Constants in the Opened Conformation of DPgn at pH 3.0. DPgn (40 µM) containing 50 mM 6-AH was titrated with 1 mM ANS over the molar ratios indicated. Top: Observed heats measured upon injection of ANS. Bottom: ANS binding isotherm resulting from integration of spikes observed during the titration. The isotherm was fit to a model involving three independent binding sites for ANS. Squares represent experimental data points while the line indicates the best fit to the experimental data.

	Compact Conformation pH 3.0			Extended Conformation pH 3.0	
K_{a1}	M^{-1}	33000 ± 2000	K_{a1}	M^{-1}	33000 ± 7000
ΔH_1	Cal/mol	-1770 ± 50	ΔH_1	Cal/mol	-1600 ± 200
ΔS_1	Cal/mol K	14.6 ± 0.3	ΔS_1	Cal/mol K	15 ± 1
$T\Delta S$	Cal/mol	4205	$T\Delta S$	Cal/mol	4320
K_{a2}	M^{-1}	360 ± 70	K_{a2}	M^{-1}	390 ± 50
ΔH_2	Cal/mol	-50000 ± 10000	ΔH_2	Cal/mol	-34000 ± 3000
ΔS_2	Cal/mol K	-160 ± 40	ΔS_2	Cal/mol K	-110 ± 10
$T\Delta S$	Cal/mol	-46080	$T\Delta S$	Cal/mol	-31680
K_{a3}	M^{-1}	6200 ± 400	K_{a3}	M^{-1}	6000 ± 700
ΔH_3	Cal/mol	-64000 ± 8000	ΔH_3	Cal/mol	-61000 ± 7000
ΔS_3	Cal/mol K	-200 ± 30	ΔS_3	Cal/mol K	-200 ± 20
$T\Delta S$	Cal/mol	-57600	$T\Delta S$	Cal/mol	-57600

Table 3: Fitted ANS Binding Parameters at pH 3.0. The binding isotherms illustrated in Figures 17 and 18 were fit to a model containing 3 independent binding sites with Origin ITC software. Results tabulated here are the average of three independent attempts to fit the data. Reported errors are the standard deviations of the averages.

Integration of the area under each deflection in the raw thermogram yields the titration isotherm. This isotherm is then fit to an appropriately selected model using the data analysis package provided with the instrument. A model involving more than one binding site was chosen to represent the ANS-DPgn system. An example of fitting results is shown in Figure 17 (bottom panel) for DPgn in the closed conformation at pH 3.0. This isotherm could not be reliably fit to a model involving a single binding site. The same was true for a model involving two binding sites. Only a model involving at least three non-interacting binding sites yielded reasonable fits. These resulting fits are listed in Table 3 (left side).

The generated fits agree well with the qualitative assessment of binding determined from fluorescence. That is to say there exists a single binding site with high affinity for ANS (low fluorescent yield) and other binding sites with weaker affinities

(high fluorescent yield). Of the three binding sites observed, the strongest binding site has a K_a of 3.3 x 10^4 M^{-1}. Binding to this site is entropically driven with a $T\Delta S$ of 4204 cal/mol. Entropy can influence the binding of nonpolar ligands in many different ways. Unfortunately, a deeper mechanistic view implied from the fitted thermodynamic variables is impossible since they reflect global events occurring between the protein, ligand and solvent (Leavitt, Freire 2001).

Two weaker binding sites also exist in DPgn as suggested by the fitting model. Listed in Table 3, these binding sites have weaker association constants of 360 M^{-1} and 6.2 x 10^3 M^{-1} respectively. Binding in both cases is enthalpically favored, but barely so. Values of $T\Delta S$ nearly compensate the drive towards bond formation, with the net binding free energy just barely driving the formation of an ANS-DPgn complex. Taken together is the noted manifestation of weaker binding constants. Despite the smaller binding constants of the weak binding sites, the associated heats of binding are substantial and well within the limits of detection of the ITC instrument. However, the uncertainties associated with fits of this class of binding sites are also substantial and may not reflect the true binding constants.

Binding of ANS to the opened conformation of DPgn at low pH is much the same as the closed conformation. The experimental results are shown in Figure 18 and the associated fits in Table 3 (right side). Qualitatively, the raw heats of binding and associated binding isotherms are practically identical to those concerning the closed conformation. The data once again fit best to a model involving three binding sites. Comparison of both data sets leads to the conclusion that the opened conformation binds

ANS with similar affinity as the closed conformation. Both conformations exhibit, within error, identical values of K_a and associated thermodynamic components.

This is not true of DPgn at neutral pH. Binding of ANS at neutral pH was much less pronounced, regardless of conformation. The experimental thermograms and associated isotherms for the closed and opened conformations of DPgn are shown in Figures 19 and 20 respectively. Fitted binding parameters are listed in Table 4.

To begin, the case for the opened conformation of DPgn is examined. Evident from Figures 19 and 20 is a marked decrease in signal magnitude at pH 6.3 compared to that observed at pH 3.0. Once again, this reaffirms the previously determined observation that ANS binding is enhanced at low pH.

Fitting the data to an appropriate model was less direct in this case. There was no a priori assumption to be made on the number of binding sites present at a pH where binding is known to be weak at best. The model of ANS binding at low pH was adopted to describe the same system at neutral pH. This model once again presumes there are three independent binding sites titrated during the course of an experiment.

From an examination of Table 4, (right side) one can see that fitting attempts were met with little success. As with the case at low pH, the same trend is followed where there exists a high affinity binding with associated K_a of 8.0×10^4 M^{-1} and two weaker sites with K_a of 2×10^3 M^{-1} and 1.3×10^4 M^{-1} respectively. However, the associated enthalpies of reaction are small, each less than 1 kcal/mol. For such cases, binding is barely evident and the fitted results do not accurately describe the system. With this in mind, one can only say that binding occurs to a very small extent at neutral pH.

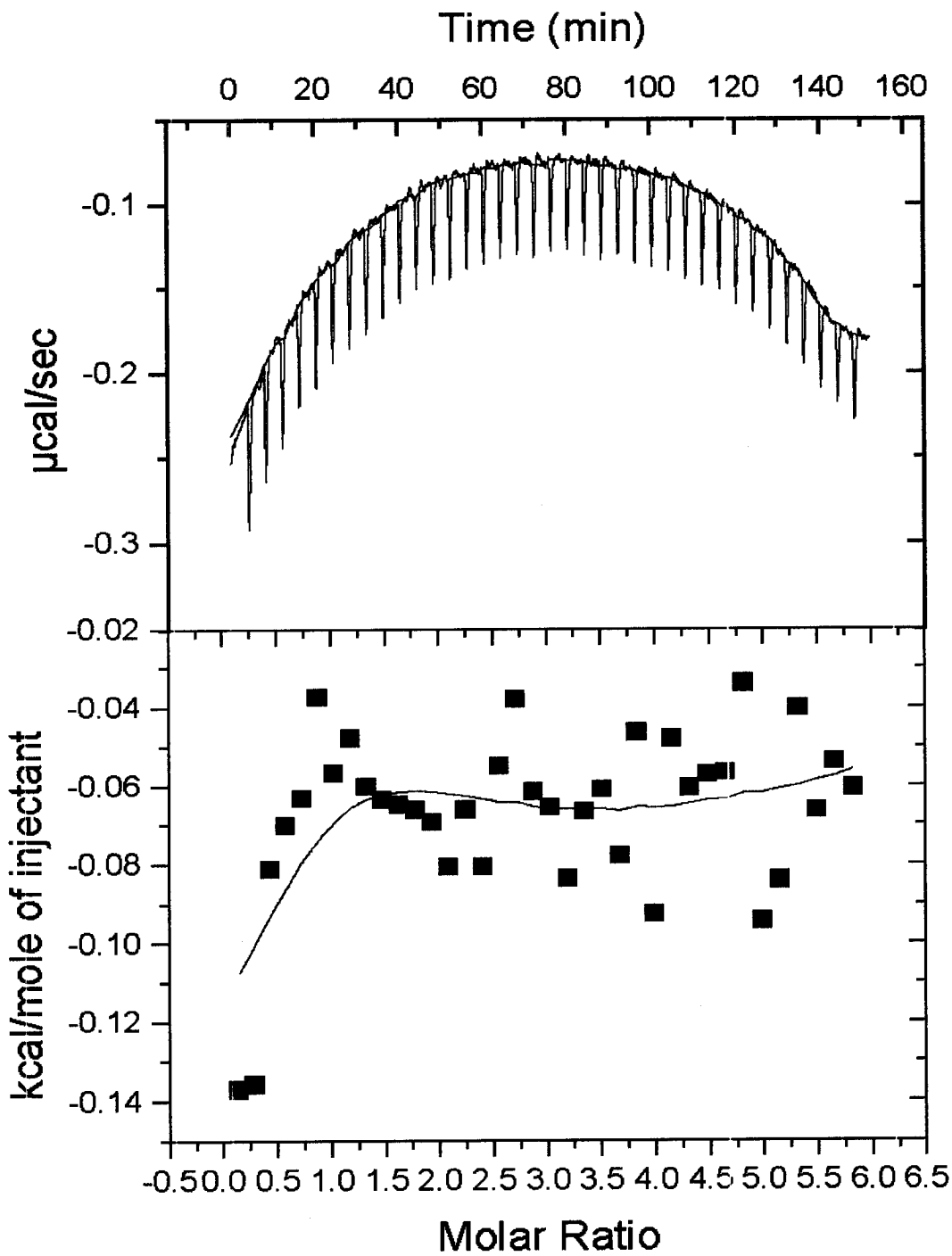

Figure 19: ITC Determination of ANS Binding Constants in the Closed Conformation of DPgn at pH 6.3. DPgn (40 µM) was titrated with 1 mM ANS over the molar ratios indicated. Top: Observed heats measured upon injection of ANS. Bottom: ANS binding isotherm resulting from integration of spikes observed during the titration. The isotherm was fit to a model involving three independent binding sites for ANS. Squares represent experimental data points while the line indicates the best fit to the experimental data.

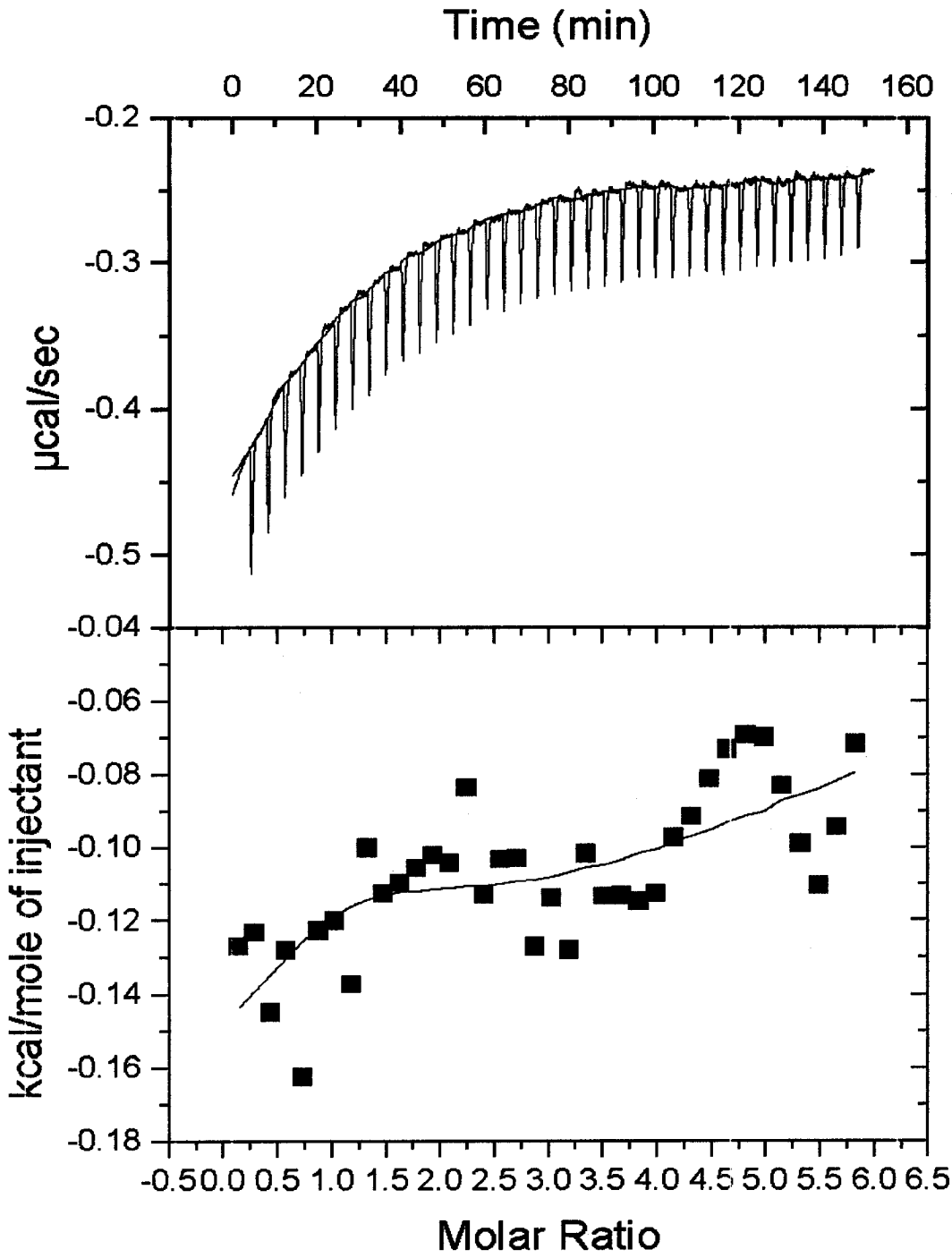

Figure 20: ITC Determination of ANS Binding Constants in the Opened Conformation of DPgn at pH 6.3. DPgn (40 µM) containing 50 mM 6-AH was titrated with 1 mM ANS over the molar ratios indicated. Top: Observed heats measured upon injection of ANS. Bottom: ANS binding isotherm resulting from integration of spikes observed during the titration. The isotherm was fit to a model involving three independent binding sites for ANS. Squares represent experimental data points while the line indicates the best fit to the experimental data.

	Compact Conformation pH 6.3			Extended Conformation pH 6.3	
K_{a1}	M^{-1}	60000 ± 40000	K_{a1}	M^{-1}	80000 ± 30000
ΔH_1	Cal/mol	-160 ± 40	ΔH_1	Cal/mol	-190 ± 20
ΔS_1	Cal/mol K	21	ΔS_1	Cal/mol K	22 ± 1
$T\Delta S$	Cal/mol	6048	$T\Delta S$	Cal/mol	6336
K_{a2}	M^{-1}	900 ± 900	K_{a2}	M^{-1}	2000 ± 200
ΔH_2	Cal/mol	-200 ± 1000	ΔH_2	Cal/mol	-930 ± 70
ΔS_2	Cal/mol K	13	ΔS_2	Cal/mol K	12 ± 1
$T\Delta S$	Cal/mol	3744	$T\Delta S$	Cal/mol	3456
K_{a3}	M^{-1}	30000 ± 30000	K_{a3}	M^{-1}	13000 ± 3000
ΔH_3	Cal/mol	-500 ± 1000	ΔH_3	Cal/mol	-150 ± 60
ΔS_3	Cal/mol K	19	ΔS_3	Cal/mol K	19 ± 1
$T\Delta S$	Cal/mol	5472	$T\Delta S$	Cal/mol	5472

Table 4: Fitted ANS Binding Parameters at pH 6.3. The binding isotherms illustrated in Figures 19 and 20 were fit to a model containing 3 independent binding sites with Origin ITC software. Results tabulated here are the average of three independent attempts to fit the data. Reported errors are the standard deviations of the averages.

The same analysis is true of DPgn in the closed conformation at pH 6.3. In this case one can see from Table 4, (left side) that reasonable fits could not be achieved within accord of the framework pertaining to a model of three binding sites. The results listed contain errors of the same, if not larger, magnitude as the fitted values of K_a and associated thermodynamic components therein. Such errors simply do not allow one to draw any inferences pertaining to the nature of ANS binding to DPgn at neutral pH. Here again, the only conclusion to be drawn is that ANS binds to DPgn with greatly diminished affinity at neutral pH.

3.5 Sedimentation Analysis of DPgn Structure With Respect to pH

Having established that ANS binds poorly to DPgn at neutral pH and remarkably well at low pH, an attempt was made to discern what structural determinants were

responsible for the enhanced binding. Sedimentation analysis was employed to examine the role of DPgn flexibility as it pertains to the binding of ANS. AUC sedimentation velocity experiments were employed to estimate the ratio of f/f_o. This information, in turn, provides information on the hydrodynamic shape of a protein in solution.

Shown in Figure 21 are results of fitted sedimentation velocity profiles under the various conditions listed in the legend. The data is represented as a c(s) distribution profile. The frequency of occurrence by which a species possesses a particular sedimentation coefficient is plotted as a function of the sedimentation coefficient to give a statistical distribution of sedimentation coefficients. The sedimentation coefficient under the peak of each envelope is the $S_{20,w}$ value listed in Table 5.

The associated sedimentation parameters for DPgn are listed in Table 5. One can see from these values that the closed and opened conformations of DPgn are readily distinguishable. At pH 6.3, the closed conformation undergoes a change in $S_{20,w}$ from approximately 5.6 S to 4.8 S for the opened conformation. This is in excellent agreement with published values of around 5.5 S and 4.4 S for the closed and opened variants of HPgn respectively (Markus et al. 1978). As such, the values reported here are acceptable and reliably distinguish the two distinct conformations.

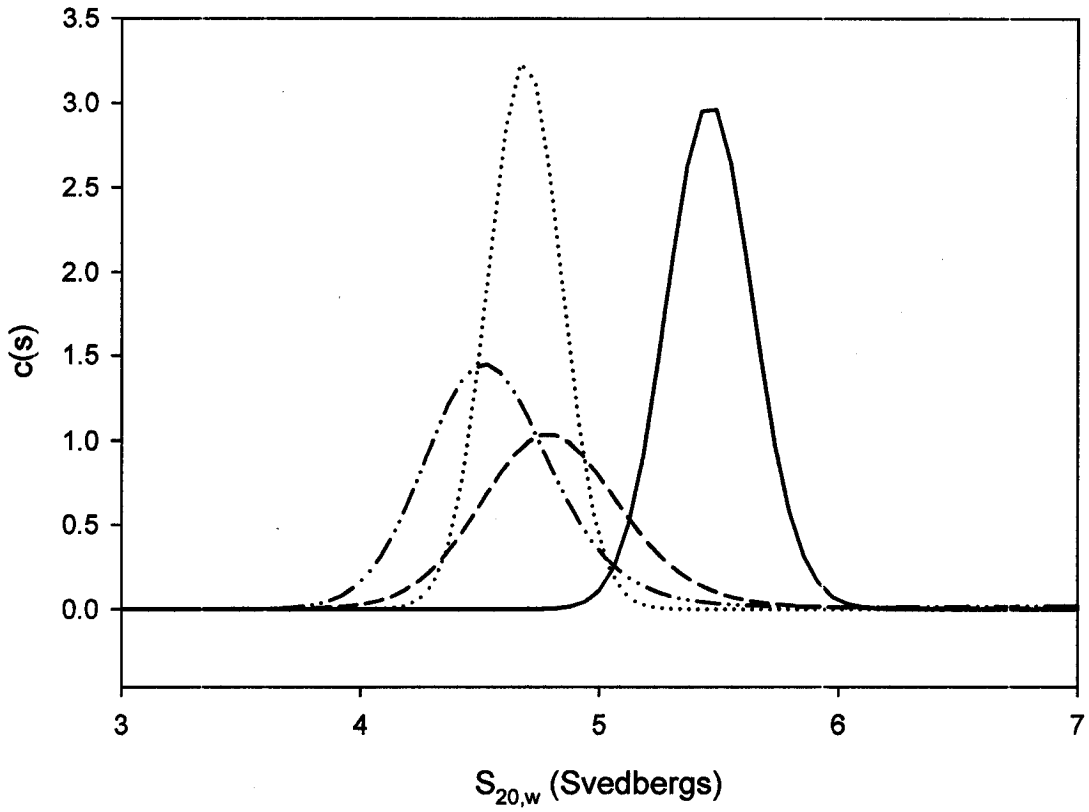

Figure 21: Sedimentation Distributions of DPgn Suggest Altered Conformations at Low pH. Shown are the sedimentation distributions obtained from sedimentation velocity runs of DPgn (6 μM) at 37 kRPM and 15 °C. Distributions were calculated using the program SedFit. The species illustrated are as follows: (Solid Line) DPgn closed, pH 6.3; (Dotted Line) DPgn opened, pH 6.3; (Dashed Line) DPgn closed, pH 3.0; (Dashed and Dotted Line) DPgn opened, pH 3.0.

Experimental pH	DPgn Conformation	$S_{20,w}$ (Svedbergs)	f/f_o
6.3	Closed	5.659 ± 0.003	1.28 ± 0.03
6.3	Opened	4.826 ± 0.005	1.50 ± 0.02
3.0	Closed	4.819 ± 0.004	1.61 ± 0.02
3.0	Opened	4.576 ± 0.003	1.62 ± 0.04

Table 5: Hydrodynamic Characteristics of DPgn as a Function of Conformation and pH. The values listed were determined from analyses of sedimentation velocity runs. Reported values are the average of five independent determinations of hydrodynamic parameters. Reported errors are the standard deviations of the averages.

The values associated with the size and hydrodynamic shapes of DPgn agree with those observed for the human variant. One can see from Table 5 that DPgn undergoes a change in f/f_o from a value of about 1.3 in the closed conformation to a value of about 1.5 in the opened conformation. In congruence from studies of HPgn (Castellino et al. 1973), this infers that the protein undergoes a change in hydrodynamic shape from that of roughly globular to less globular upon binding 6-AH.

More interesting is the hydrodynamic behavior of DPgn at low pH. From Table 5 it is evident that the $S_{20,w}$ values for both conformations of DPgn at pH 3.0 resemble the opened conformation at pH 6.3. This is interpreted to mean that at low pH DPgn preferentially adopts a structure resembling the opened conformation. This occurs even in the absence of 6-AH, a condition which would otherwise favor the closed conformation.

A comparison of f/f_o ratios also suggests an altered symmetry of DPgn at low pH. One can see from Table 5 that at pH 3.0 the ratio of f/f_o increases to a value of roughly 1.6 whether 6-AH is present or absent. This indicates that at pH 3.0, DPgn adopts a more extended hydrodynamic shape regardless of 6-AH presence. Here again, this is taken to mean that the protein undergoes a conformational change towards the opened conformer as pH is decreased.

The values of f/f_o at pH 3.0 are not identical to the opened conformation of DPgn at pH 6.3. At pH 6.3, the opened conformation of DPgn exhibits a value of f/f_o equal to 1.5. At pH 3.0, both conformations of DPgn have similar values of f/f_o being roughly equal to 1.6. Within error, this value of 1.6 is greater than that of the opened conformation at pH 6.3. This is possibly due to expansion of the hydrophobic core at

such an extreme pH. The idea of hydrophobic expansion agrees well with the observed increase in ANS fluorescence emissions when bound to DPgn at low pH.

3.6 Tertiary structure of DPgn is Altered as a Function of pH

Sedimentation velocity analysis indicated that DPgn undergoes a conformational change in response to a decrease of pH. It is likely that this conformational change is identical to that experienced upon binding 6-AH; the change from a compact, closed conformation to an extended, open conformation. Near-UV circular dichroism (CD) is another useful method to examine changes in tertiary structure. The technique was used to complement data obtained through sedimentation analysis.

Shown in Figure 22 is a CD spectrum of DPgn in its native, closed conformation at pH 6.3 and at pH 3.0. There are marked differences between the two spectra. The native spectrum shows well defined CD structure in the aromatic region. Such structure is due primarily to the aromatic amino acid residues folded into an asymmetric environment within the overall protein fold.

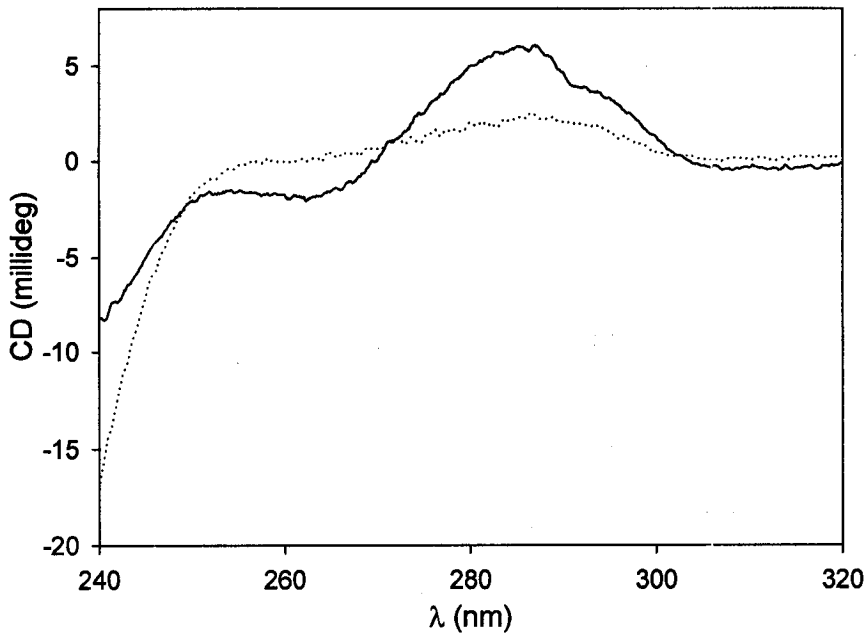

Figure 22: Tertiary Structure of DPgn Changes as a Function of pH. Shown is a near UV CD spectrum of DPgn (10 μM) in the closed conformation at either pH 6.3 (solid line) or pH 3.0 (dotted line). There is a loss of CD signal at pH 3.0 compared to the spectrum observed at pH 6.3. This suggests an altered conformation of DPgn at low pH.

The spectrum of DPgn at pH 3.0 shows an attenuated CD signal in the aromatic region. When compared to the spectrum at pH 6.3, it is obvious that there are differences. The loss of CD signal in this context is interpreted to mean that the tertiary structure of DPgn at pH 3.0 differs from that observed at pH 6.3.

Unfortunately, one cannot infer a deeper insight into structural differences between the two conformers of DPgn from the illustrated CD spectra alone. In this case, loss of CD signal may or may not mean that the aromatic residues are relocated into a more symmetric environment upon a decrease in pH. The CD signal for an aromatic residue can be either positive or negative (Kahn 1979). As such, there are no a priori assumptions one can make about the spectral behavior of the aromatic residues upon changes in environment. This taken together with the fact that DPgn contains over 70

aromatic residues makes such an inference impossible. All that can be said is that the asymmetric environment experienced by aromatic residues differs between the pH values examined. In light of DPgn structural dynamics, this agrees with the findings afforded from sedimentation analysis.

3.7 Localization of ANS Binding Sites

Having established that ANS binds to DPgn under conditions of low pH, it is desirable to determine where it binds. In doing so, one might infer the topographic regions within DPgn which become exposed at low pH. To this end, proteolytic digestion of DPgn by porcine elastase, followed by native PAGE and ANS staining was examined.

To begin, optimized conditions for proteolysis were determined from trials involving DPgn digestion at different time intervals. The results of such trials are shown in Figure 23 after SDS-PAGE development. It can be seen that after one hour (lane 4), digestion has proceeded to a large extent. Overnight digestion (lane 7) yields similar digest patterns. Proteolysis appears to be complete after overnight digestion. Furthermore, nonspecific cleavage of DPgn is minimal despite the lengthy digestion time since similar peptides are observed after one hour. For these reasons, subsequent experiments were incubated overnight to allow for complete digestion.

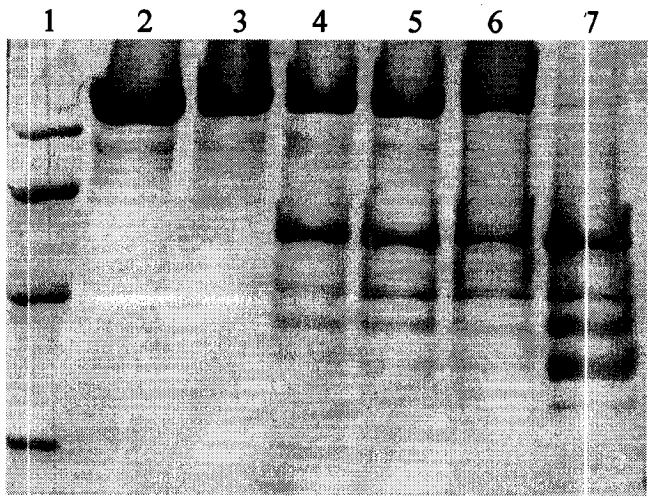

Figure 23: Elastase Digestion Conditions: DPgn (5 mg) was proteolytically digested with porcine elastase at an enzyme:substrate ratio of 1:100 (w/w). Digestion proceeded at room temperature for the time intervals listed. Lane 1: Molecular weight markers; Lane 2: Native DPgn control after 1 hour; Lane 3: Native DPgn control overnight; Lane 4: DPgn Digest after 1 hour; Lane 5: Digest 2 hour; Lane 6: Digest 3 hour; Lane 7: Overnight Digest. Elastase only control not shown. Molecular weight markers were from BioRad: (Top to Bottom): phosphorylase b (97.4 kDa), BSA (66.2 kDa), ovalbumin (45 kDa), carbonic anhydrase (31 kDa), trypsin inhibitor (21.5 kDa, not shown), lysozyme (14.4 kDa, not shown).

Purification of the overnight digestions was achieved by affinity chromatography using a lysine-Sepharose matrix. Results of a purification are shown in Figure 24 (top panel) after ANS staining at pH 3.0. The purification yields two fractions. First, a wash fraction was obtained (Lane 3). This fraction did not bind to the lysine-Sepharose resin and probably contains proteolytic fragments void of lysine binding sites. These peptides likely are free of functional kringle domains. The second fraction (Lane 4) remained bound to the Lysine-Sepharose matrix until elution with excess 6-AH. Therefore, this fraction must possess functional lysine binding sites typical of kringle domains.

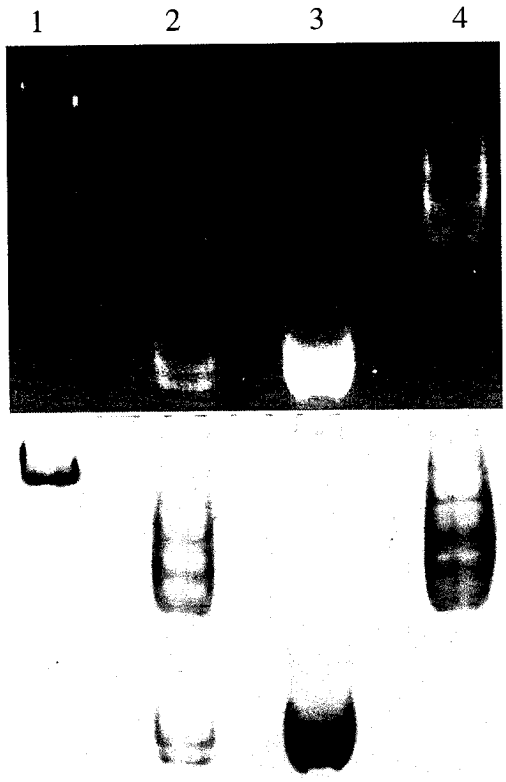

Figure 24: Purified Elastase Cleavage Products of DPgn Bind ANS.
Top Panel: Overnight cleavage products of DPgn (5 mg) were separated on Lys-Sepharose and developed in a 10% native gel, followed by subsequent staining in ANS (1 mM) at pH 3.0. Lane 1 contains undigested DPgn. Lane 2 contains the overnight digest products. Lane 3 contains the flowthrough portion that did not bind to Lys-Sepharose. Lane 4 contains the portion which bound to Lys-Sepharose. Each lane contained approximately 15 μg total protein. Bottom Panel: Coomassie stain of the same gel indicating identical staining patterns.

Both purified fractions bound ANS. From Figure 24, (top panel) it is noted that ANS binds to the kringle void fraction as well as to the kringle containing fraction. It is unlikely that previously unexposed ANS binding sites were artificially introduced due to the fact that ANS fluorescence was absent when stained at pH 6.3 (data not shown). Therefore, the pattern obtained at pH 3.0 is believed to be representative of fragments possessing identical binding sites as was probed in previous experiments.

Binding of ANS to the purified proteolytic fragments gives information on the minimum number of binding sites available. Since both purified fractions exhibited ANS

fluorescence at pH 3.0, it is straightforward to assume that there are at least two binding sites available on an intact DPgn molecule. This agrees with the observations obtained from ITC in that DPgn binding isotherms could be fit only to a model containing a minimum of three binding sites. The evidence provided here corroborates this claim in that at least two of these binding sites are justified.

Subsequent to determining the minimum number of ANS binding sites, an attempt was made to localize the sites to regions within the DPgn topography. This requires knowledge of what fragmentation patterns one would expect upon complete digestion. Before analyzing the obtained digestion patterns in greater detail, the focus will shift to the known fragmentation patterns of the human variant, HPgn.

Figure 25 illustrates a schematic representation of HPgn based on known elastase cleavage sites as reported by Sottrup-Jensen (Sottrup-Jensen et al. 1978). In this figure, HPgn is represented as a shaded box. The numbering above the box refers to the positions of residues known to be cleaved by elastase. Under the box are enlarged regions showing the primary sequence of HPgn (top lines) flanking the cleavage site. The bottom lines within the enlargements indicate the homologous regions of DPgn. The cleavage sites are marked within the specified sequences in bold type font. Also indicated are regions of the DPgn sequence whose sequence is currently unknown. These regions were substituted with the homologous HPgn sequence and are underlined as indicated.

Above the shaded box of Figure 25 is a map illustrating the domains contained within the holoprotein. The map is aligned to indicate relative positions of each domain with respect to cleavage sites. Primary cleavage sites are located within loops flanking

the kringle domains specified. Upon cleavage, the patterns indicated below the shaded box arise.

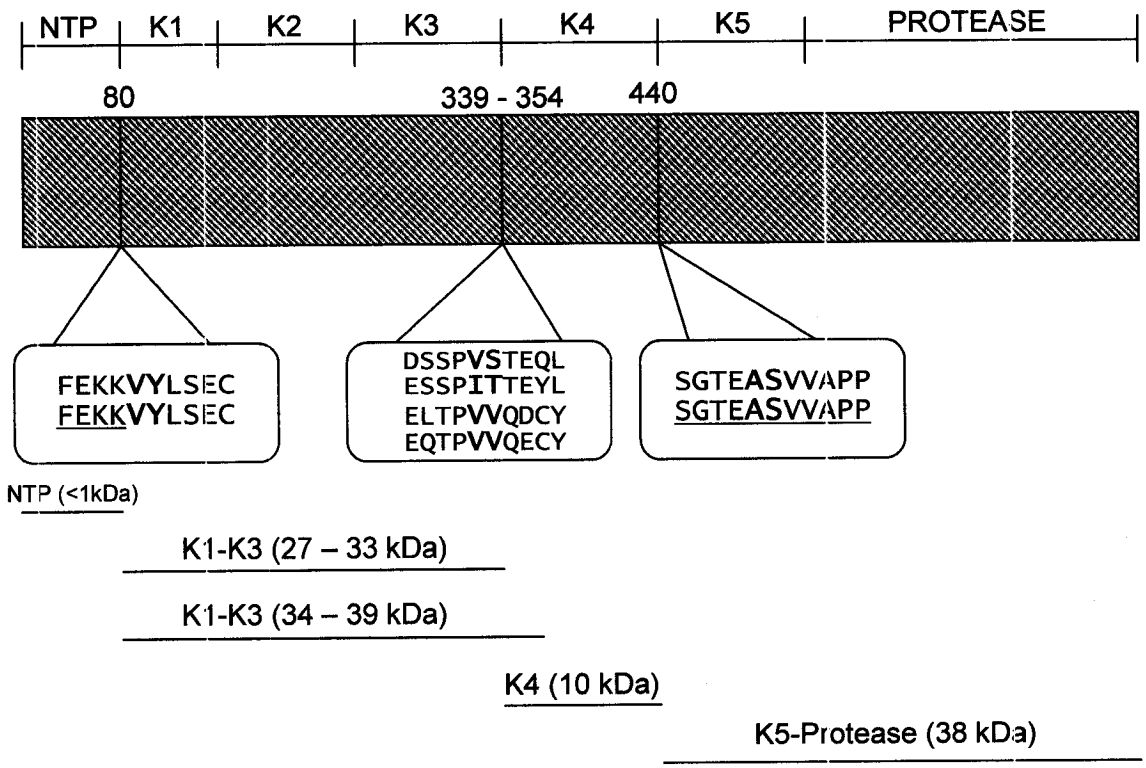

Figure 25: Schematic of HPgn Illustrating Known Cleavage Sites for Elastase.
HPgn is represented as the shaded box. Below the box are enlarged views of known elastase cleavage sites showing the primary sequence flanking each cut site. The cut sites are shown in bold typeface. Below the indicated HPgn sequences (top sequence) are the homologous sequences of DPgn (bottom sequence). Where the DPgn sequence was unknown, the HPgn sequence was inserted. The unknown sequences are underlined. Two cleavage sites exist between residues at position 339 and 354 and are indicated in the middle box. Indicated at the bottom of the figure are the expected sizes of cleavage products.

In practice, cleavage of HPgn gives rise to three primary fragments visible by SDS-PAGE. These fragments are comprised of kringles 1-3, kringle four and a fragment containing kringle five connected to the protease domain. As indicated in Figure 25, kringles 1-3 give rise to more than one fragment. This heterogeneity results from differences in the extent to which the various isoforms of Pgn are glycosylated. For this

reason, one expects the fragments containing kringles 1-3 to yield multiple bands on SDS-PAGE gels.

The size distribution of fragments obtained from elastase cleavage is well characterized. Fragments as noted in Figure 25 are to be expected from HPgn and are easily identified on gels. DPgn should yield similar digestion patterns whose fragments would have a similar distribution of sizes.

The purified fragments obtained from elastase cleavage of DPgn were developed by SDS-PAGE. Shown in Figure 26 (top panel) are the fragmentation patterns obtained under non-reducing conditions. Under these conditions, disulfide bonds remain intact simplifying the identification of bands. Listed in Table 6 are the size distributions of the bands.

The lysine-Sepharose flowthrough portion is contained in lane four. There are four readily identified bands possessing molecular weights of 44 kDa, 39 kDa, 36 kDa, and 29 kDa respectively. In congruence with the assignments determined by Sottrup-Jensen et al, it is likely that the 36 kDa and 39 kDa bands are variants of mini-DPgn. The bands above and below mini-DPgn cannot be assigned in that their molecular weights (44 kDa and 29 kDa) do not fall within the ranges observed for HPgn.

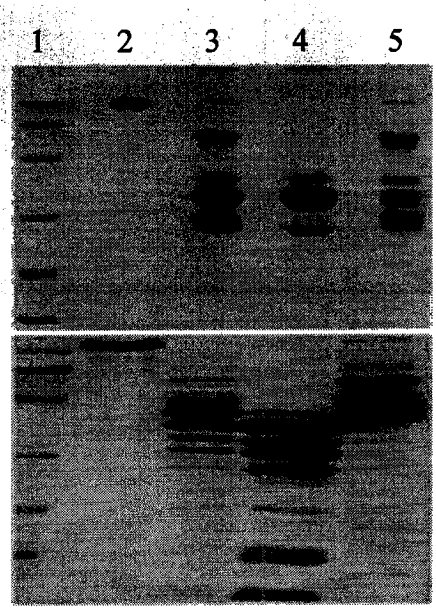

Figure 26: Identification of Elastase Digest Products: SDS-PAGE was used to estimate the sizes of fragments obtained from elastase digestion. Top: Non-Reducing 10% Gel. Lane one contains molecular weight markers whose sizes are indicated in Figure 23. Lane two contains undigested DPgn. Lane three contains unpurified fragments from an overnight elastase digest. Lane four contains Lys-Sepharose flowthrough. Lane five contains fragments bound to Lys-Sepharose. Bottom: Reducing 10% Gel. The lane identities are identical to the non-reducing gel. Both gels contain 15 μg total protein loaded per lane. Molecular weight markers are as defined in Figure 23.

Kringle containing fragments which remained bound to lysine-Sepharose are shown in lane 5. The fragments yield molecular weights of 62 kDa, 44 kDa, 38 kDa and 32 kDa respectively (Table 6). It is likely that the 38 kDa and 32 kDa bands are variants of the kringle 1-3 containing fragments. The band at 62 kDa is possibly a fragment containing multiple kringles connected to the protease domain, however this remains uncertain. Finally, the band at 44 kDa also remains uncertain and the identity thereof was not assigned.

Fraction	R_f	M_r (kDa)	Assigned Identity
Undigested DPgn	0.13	81.1	Native DPgn
Lys-Sepharose Flowthrough	2.05	43.8	Unknown
Lys-Sepharose Flowthrough	2.30	38.8	Mini-DPgn
Lys-Sepharose Flowthrough	2.45	36.1	Mini-DPgn
Lys-Sepharose Flowthrough	2.89	29.2	Unknown
Lys-Sepharose Bound	1.32	62.2	Multiple Kringle-Protease
Lys-Sepharose Bound	2.03	44.2	Unknown
Lys-Sepharose Bound	2.32	38.4	K1-K3
Lys-Sepharose Bound	2.70	32.0	K1-K3

Table 6: Size Estimates of Elastase Digest Fragments. Listed are the estimated sizes of elastase digest fragments as were developed under non-reducing conditions. Estimates were made by measurements of R_f values and a standard curve generated from molecular weight standards.

Attempts were also made to develop the purified fractions under reducing conditions. Results from such an experiment are shown in Figure 26 (bottom panel). The reduction of disulfides generates many bands. This means that elastase cleaves DPgn in many locations. Since DPgn contains a large disulfide network, it retains a greater degree of tertiary structure under non-reducing conditions. Due to the underlying complexity of this network, assignment of each band under reducing conditions was not investigated further.

4.0 Discussion

4.1 Plasminogen Binds ANS at Low pH

The work presented in Section 3 illustrates that under appropriate conditions, the canine variant of plasminogen binds the fluorescent probe, ANS. Conditions favoring binding occur at low pH. At neutral pH binding occurs, but does so with a remarkably diminished magnitude. This was established qualitatively through examination of ANS stained native PAGE gels.

At pH 3.0, ANS binding could be distinguished due to an increased fluorescence signal compared to the background (Figure 13). Identical patterns were observed when the gel was subsequently stained in Coomassie Blue. This confirmed that ANS-bound DPgn was responsible for the fluorescent bands observed in the gel. Furthermore, the fluorescent patterns observed at pH 3.0 were not visible at pH 6.3 confirming that pH plays a dominant role in ANS binding.

Similar trends were observed through examination of steady-state fluorescence titrations (Figures 15 and 16). At neutral pH, ANS binding was very weak, judging by the increase in fluorescence emission at 470 nm. Conversely, binding at pH 3.0 was enhanced as witnessed by a much larger increase in fluorescence emission compared to that observed at pH 6.3. Again, the trend towards enhanced binding at low pH is noted.

It was shown that binding occurred at neutral pH, but became markedly enhanced at low pH (Figure 16). Fluorescence emissions at a constant molar value (ANS/DPgn) did not change much with pH until below pH 4.0. Below pH 4.0, the emissions increased dramatically.

Finally, the trend towards preferential binding at low pH was confirmed with ITC. Binding isotherms were well defined at pH 3.0 (Figures 17 and 18). However, at pH 6.3, the measured signals due to ANS binding were too small to reliably detect. As a result, binding could only be characterized at pH 3.0. It is concluded that binding occurs to only to a minor extent at neutral pH.

4.2 Binding Occurs at Multiple Binding Sites

The fluorescence titrations shown in Figure 15 are indicative of multiple binding sites. At the earlier parts of the titration there is a response likely due to a strong binding site with a small fluorescence yield. While binding at this site is strongest, its saturation is not evident due to the larger fluorescent yields of secondary sites.

The strongest binding site corresponds to the site saturating at a molar ratio of about one as observed in the ITC isotherms at pH 3.0 (Figures 17 and 18). This site binds ANS with an associated binding constant of about 3×10^4 M^{-1} (K_d = 30 μM). This also agrees with the noted deviation from linearity, occurring at about the same molar ratio in the fluorescence titrations (Figure 15). For example, at a molar ratio (ANS/DPgn) of about 2 there was a notable deviation from linearity observed from the fluorescence binding curves. Similarly, the ITC binding isotherms show an initial plateau region upon reaching a molar ratio of 1 and the fitted binding parameters associated with this plateau likely reflect the same deviation observed from the fluorescence titrations.

According to the ITC data fits, the driving force for binding at this site is an overall increase in entropy. Unfortunately, the exact manner by which entropy influences the binding cannot be assigned. Binding events driven by entropy result in an overall

increase of disorder for the system concerned. The system considered here is complex. One must account for increases in disorder between DPgn, ANS and solvent waters. Without further structural knowledge, such an assignment is impossible.

Secondary binding sites begin to fill later in the titration. These binding sites have a large fluorescence yield and bring about the upward curvature noted in the latter parts of the pH 3.0 isotherm in Figure 15. Based on the exaggerated fluorescence yield after saturation of the strong binding site, it seems possible that these sites are less hydrated in the bound state and thus give rise to the larger fluorescence enhancement.

Secondary sites were also observed to have a considerably weaker affinity towards ANS as observed through ITC. The second weakest binding site with an associated K_a of 6 x 10^3 M^{-1} (K_d = 160 μM) only began to saturate by the end of the experiment. Meanwhile the weakest site with associated K_a of 360 M^{-1} (K_d = 2.8 mM) was barely sampled at all. Uncertainty associated from extrapolated data fits of the weakest binding site precludes an accurate characterization. Despite this shortcoming, the ITC data confirm the observation of multiple binding sites within a DPgn molecule.

The driving forces governing binding at the secondary sites are balanced with a slightly larger enthalpic contribution. Binding is driven by an overall decrease in the energy of the system. However, the precise manner by which enthalpy drives the reaction cannot be determined due to insufficient structural detail. Furthermore, the enthalpic contribution towards the determined binding constant is nearly compensated by an unfavorable entropic drive towards disorder. This compensation results in the observation of weaker binding at these sites.

The identification of multiple ANS binding sites at low pH was ultimately established through examination of elastase digest fragments. Separation of the fragments into two pools allowed for visualization of the sites. Subsequent identification from SDS-PAGE suggested that the kringle containing, angiostatin-like fragments, as well as the proteolytic domain bind ANS. As such, the assumptions made upon choosing a model involving three binding sites is not unreasonable. However, while it is reasonable to believe that three binding sites exist, the existence of other sites cannot be excluded. Unfortunately, the resolution afforded by gel electrophoresis precludes the possibility of identifying such sites.

4.3 ANS Binds to the DPgn Proteolytic Domain

Results obtained from electrophoresis of elastase digest fragments suggested that the proteolytic domain contains at least one of the binding sites observed for ANS. This result is not surprising. It closely parallels the knowledge that chymotrypsin binds ANS.

Mentioned briefly in the introduction was a study where ANS was observed to bind to a site in chymotrypsin (Weber et al. 1979). The crystal structure determined in this study revealed that the ANS binding site was not at all hydrophobic. The binding site was located in a solvent exposed region containing a disulfide between Cys1 and Cys122 and surrounded by an array of charged residues. Located in HPgn is a similar disulfide between Cys548 and Cys666 (Terzyan et al. 2004). Alignment of the HPgn proteolytic domain with chymotrypsin yields similar placement of the disulfides located within a nearly identical space. The RMS deviation is less than 2 Å, suggesting that Pgn should contain an identical binding site for ANS.

The similar binding site in chymotrypsin bound ANS with an associated K_d of around 140 μM at pH 3.6. The secondary binding sites observed from the ITC titrations may reflect a similar binding site. The observed K_d of 160 μM is reasonably similar to that noted for chymotrypsin. This probably reflects the binding site observed to be contained within the proteolytic domain.

To further illustrate the similarity with chymotrypsin, Weber et al. also noted an identical dependence of ANS fluorescence emissions with pH. At pH 3.6 ANS fluorescence was far greater in comparison to the marginal fluorescence at pH 6.9. Since the ANS binding site was solvent exposed and not hydrophobic, a role for water was proposed where the conformation of chymotrypsin at pH 3.6 exhibited an ANS binding site containing ordered water molecules. This conformation differed very little from that determined at physiological pH. The ordered water molecules around the bound ANS induced a conformation of ANS such that the phenyl moiety adopted a unique geometry. This induced geometry and altered water mobility around the binding site resulted in the notable increase of fluorescence lifetimes.

Meanwhile at pH 6.9 the same region experienced a higher mobility of water resulting in quenched ANS fluorescence. The net result was similar to that observed with DPgn, a drastically reduced fluorescence lifetime. The findings observed with chymotrypsin probably apply to a similar binding site within DPgn.

4.4 The NTP May Prevent ANS Binding in a Closed Conformation

Unfortunately, in this analysis one cannot account for the exact location of the NTP with respect to the proteolytic domain. There is no way of knowing if it would

hinder binding of ANS to the homologous region known to bind ANS in chymotrypsin. It is known that kringle 2 overlaps the proteolytic domain in the closed conformation of HPgn (Banyai, Patthy 1985). This was determined by introduction of a chemical cross link between Lys203 of kringle 2 and Tyr671 of the protease domain.

The distance between Tyr671 and Cys666 is on the order of 15 Å. There is a reasonable separation. Manipulation of the crystal structures for kringle 2 and the proteolytic domain allow one to envision the cross linkage between Lys203 and Tyr671. Exploration of different fits between the two proteins is instructive. In doing so it is necessary to maintain the location of residues known to cross-link within a distance favoring their contact. A few conformations can be generated where the proposed ANS site is totally blocked by kringle 2.

The homologous residues of HPgn which could yield a functional ANS binding site as observed in chymotrypsin are also observed in DPgn. Located at positions 550 and 668 in DPgn are Cys residues. Taken together with the fact that the DPgn proteolytic domain is also a serine protease, the disulfide formed therein is probably located in similar positions upon folding. It is therefore reasonable to assume that the observed binding site in the proteolytic domain is similar to that observed in chymotrypsin.

The position of this binding site relative to kringle 2 in the closed conformation cannot be determined. The evidence presented here suggests that ANS does bind to the proteolytic domain. At neutral pH, it is entirely possible that the binding site is in fact concealed by the NTP. If so, one would expect the site to become exposed in the opened conformation. This was not observed. The observed heats of ANS binding were unreliably small in both conformations of DPgn at pH 6.3. Meanwhile, the observed

heats at pH 3.0 were substantially larger, but independent of the protein conformation. One cannot eliminate the possibility that the proposed protease binding site is concealed by the NTP in the closed conformation. However, the evidence provided here suggests otherwise.

4.5 Binding Does Not Occur Within Lysine Binding Sites

The lysine binding sites of Pgn contain a hydrophobic component that favorably interacts with the methylene subunits of lysine and lysine analogs. One might expect ANS to bind within such sites in which case fluorescence enhancement could be due to shielding of the naphthalene ring system from water. If so, the presence of saturating amounts of 6-AH would diminish the fluorescence. This was not observed in either conformation of Pgn as illustrated from ITC titrations. At pH 3.0, both conformations of Pgn, were shown to bind ANS with similar affinities (Table 3). The presence of 6-AH in no way affected binding of ANS and thus it is concluded that ANS binds to a region removed from the lysine binding sites.

On the other hand, it is possible that at pH 3.0, binding of 6-AH to the LBS is diminished. The known pK_a's of 6-AH are 4.31 and 10.81 for the carboxyl and amino termini respectively. At pH 3.0, the amino group is most certainly protonated while the carboxyl group is partially protonated. Similarly, the electrostatic determinants contained within the LBS are protonated to a greater extent at pH 3.0. This probably affects binding of 6-AH at each respective LBS. In fact, the conformation of DPgn at pH 3.0 in the absence of 6-AH might be extended due to diminished ligation of the NTP. Indeed, this was suggested from the $S_{20,w}$ and f/f_o values measured in the sedimentation analysis.

4.6 Enhanced Binding of ANS is Accompanied by Changes in DPgn Flexibility

Large changes in the sedimentation profiles of DPgn were observed as a function of pH. Readily observable was the conformational change from the closed to opened form at pH 6.3. The results presented here were in excellent agreement with published values. Upon binding 6-AH, DPgn undergoes a change in shape from roughly spherical, to the more extended shape associated with the opened conformation. This change of symmetry was reflected in the fitted frictional ratios. While the closed conformer exhibited a ratio of approximately 1.3, the opened conformer exhibited a value of 1.5.

At pH 3.0, the sedimentation of DPgn reflects the opened conformation at pH 6.3. It is evident from the f/f_o ratios that at pH 3.0 DPgn is more extended. At this pH, the designation of the closed conformer is inaccurate. The frictional ratio of the closed conformer at pH 3.0 more closely resembles that of the truly opened conformer at pH 6.3. The c(s) distributions in Figure 21 illustrate this. At pH 3.0 there is a larger population of species sedimenting in a manner identical to the opened conformer at pH 6.3. This distribution overlaps that of the closed conformation at pH 6.3 only marginally. As such, DPgn mainly adopts a more extended conformation at low pH, similar to that of the opened conformation at neutral pH. This interpretation agrees well with the fact that a lysine binding site is responsible for ligating the closed conformation of Pgn.

The extended conformation of DPgn at low pH is likely more extended than that of the opened conformer at neutral pH. From Table 5 one can see that the frictional ratios of DPgn at low pH are significantly larger than the corresponding ratio of the opened conformer at neutral pH. This makes sense taking into account that at low pH a protein adopts a primarily positive charge due to protonation of its acidic amino acid sidechains.

Upon protonation there will be a net repulsion from protonated basic amino acids. This leads to an expansion of the protein's hydrodynamic radius as is reflected in the sedimentation data presented here.

4.7 Errors Inherent in Sedimentation Analysis

The sedimentation analysis presented here incorporates assumptions. The first assumption refers to the value calculated for the partial specific volume of DPgn. This value, 0.7165 at 15 °C, was calculated from the reconstructed sequence of DPgn using the program Sednterp. The chimeric nature of this sequence introduces error since regions of the human variant were introduced. These regions account for less than 10% of the entire DPgn sequence. Until the entire sequence is determined, there is no way of knowing if this is correct.

The calculated value of v-bar requires knowledge of this sequence. Use of a chimeric sequence introduces uncertainty. This is unavoidable. However, this uncertainty is probably less than 1% considering that all known mammalian Pgn sequences share approximately 90% identity. To illustrate this, the calculated v-bars for the human and canine variants at 25 °C are 0.7194 and 0.7207 respectively. The difference between the two values is small, suggesting that the calculated v-bar of DPgn does not introduce a large degree of uncertainty.

A larger degree of uncertainty is introduced due to the dependence of v-bar with pH. For example, BSA undergoes a change in v-bar from a value of 0.73 at pH 6 to a value approaching 0.70 at pH 2 (Durchschlag, Jaenicke 1982). To complicate matters further, a determination of v-bar for a protein requires both a large amount of material as

well as equipment capable of high precision. To get around this, many investigators choose simply to calculate v-bar from sequence data.

At neutral pH this is probably a reasonable approach. On the other hand, at low pH, the calculated value for v-bar may not truly reflect the nature of the species being investigated. Again, this is unavoidable and introduces a degree of uncertainty. The magnitude of this uncertainty is unknown. Regardless, the sedimentation analysis of the species at low pH is in general agreement with the other methods discussed and is considered valid in the context of this analysis.

4.8 Altered Tertiary Structure of DPgn at Low pH

The sedimentation behavior of DPgn at low pH suggests that it experiences greater flexibility than at neutral pH. This was also observed in the near UV CD spectra of DPgn at pH 3.0 and 6.3. The spectra presented in Figure 22 suggest that at pH 3.0 DPgn exhibits a different conformation than at pH 6.3. It was concluded that while the CD signal decreases at pH 3.0, this can not necessarily be attributed to a loss of tertiary structure. This may be true, but one can only say that the conformation is indeed different at pH 3.0. This conformation corresponds to the expanded conformation also observed in the sedimentation analysis. It is this altered conformation that preferentially binds ANS.

4.9 Increased Flexibility at Low pH and the Molten Globule

Structural expansion of a protein at low pH must impart a greater degree of structural freedom with respect to maintaining a native fold. Repulsive forces exerted by

protonated basic amino acids likely allow a protein to explore alternative folds which are similar in structure, but not identical to the native fold. Such alternative conformers would not be as tightly packed as in the native state. Weaker packing of the interior domain of a protein ultimately yields a structure with a more exposed hydrophobic core. This is exactly the type of structure to which ANS preferentially binds.

It is possible that DPgn unfolds through the pathway of a molten globule. This would explain the preferential binding of ANS at low pH. Sedimentation data corroborates this notion with the observed increase in protein flexibility at low pH. Regardless, this interpretation requires further knowledge. For example, denaturant induced unfolding profiles of reduced DPgn must be compared at pH 3.0 and 6.3. Positive evidence towards the assignment of a molten globule occurs if the transition to a completely unfolded state is attenuated at low pH.

Comparison of time resolved fluorescence profiles would also allow one to determine if ANS binds to a native protein structure. It has been suggested that ANS bound to a native protein yields shorter fluorescence lifetimes ($\tau \sim 11$ ns) compared to molten globule-bound ANS ($\tau \sim 16$ ns) (Uversky et al. 1998). Data of this sort, taken together with denaturation profiles would provide reasonable evidence towards the identification of a molten globule at low pH.

4.10 Buffer Conditions Influence ANS spectral Properties

To be thorough, it is necessary to point out that the spectral properties of ANS likely change as a function of pH. Contained at position one of the naphthalene ring system in ANS (Figure 10) is a sulfonyl functional group. The pK_a of this group has not

been established, but has been suggested to remain deprotonated under the acidic conditions that often lead to protein denaturation (Matulis et al. 1999;Uversky et al. 1998;Weber et al. 1979).

It might be expected that the charge of the sulfonyl moiety of ANS affects its fluorescence yield. This is reflected in the observed increase of the fluorescence yield of free ANS at low pH (Figure 16, inset). As such, there is perhaps a small contribution towards enhanced binding to DPgn due to the degree of protonation of the sulfonyl moiety of the ANS ring system. Despite this, it is obvious that introduction of DPgn dramatically enhances the fluorescence yield beyond that which was due to protonation of the sulfonyl group. Thus, binding is only marginally enhanced due to ANS protonation and is markedly enhanced due to the structural changes induced in DPgn at low pH.

The matter of buffer composition is further complicated when ionic strength is considered. Table 1 lists the calculated ionic strengths of the buffers used when examining ANS binding as a function of pH. The ionic strength of the citric acid-phosphate buffer system increases by a factor larger than two as one proceeds from pH 3.0 to 6.0 (Figure 16, inset). In an inverse manner, the fluorescence yield decreases as one proceeds from pH 3.0 to 6.0. Though the magnitude of these changes is not identical, it cannot be ruled out that ionic strength plays a role in the fluorescence of free ANS. Binding of ANS to DPgn is possibly affected by ionic strength. If so, the effect is only marginal; the gross conformational properties of DPgn play a much larger role in binding.

4.11 Concluding Remarks

Throughout this study, it was shown that DPgn binds ANS under conditions of low pH. Binding occurred primarily at low pH as noted by enhanced fluorescence and ITC. More than one binding site for ANS is observed. One such site is likely contained within the proteolytic domain of DPgn. Binding most likely occurs to an altered conformation of DPgn. This conformation is more flexible at low pH than and more closely resembles the opened conformation observed at pH 6.3. The enhanced flexibility at low pH ultimately exposes binding sites for ANS. Some of these binding sites are probably contained within the hydrophobic core of DPgn. As such, it is likely that ANS binds preferentially to a molten globule form of DPgn rather than the native conformation.

Reference List

Abad,M.C., Arni,R.K., Grella,D.K., Castellino,F.J., Tulinsky,A., and Geiger J.H. 2002. The X-ray Crystallographic Structure of the Angiogenesis Inhibitor Angiostatin. *Journal of Molecular Biology* **318**:1009-1017.

American Heart Association. *Heart Disease and Stroke Statistics - 2004 Update*. 2004. Dallas, TX, American Heart Association.
Ref Type: Report

An,S.S., Carreno,C., Marti,D.N., Schaller,J., Albericio,F., and Llinas,M. 1998. Lysine-50 is a likely site for anchoring the plasminogen N-terminal peptide to lysine-binding kringles. *Protein Sci.* **7**:1960-1969.

Banyai,L. and Patthy,L. 1985. Proximity of the catalytic region and the kringle 2 domain in the closed conformer of plasminogen. *Biochim. Biophys. Acta* **832**:224-227.

Bino J., D'Silva P.R., and Lala A.K. 2001. Analysis of protein folding using polarity-sensitive fluorescent probes. *Current Science* **80**:287-290.

Castellino,F.J. 1984. Biochemistry of human plasminogen. *Semin. Thromb. Hemost.* **10**:18-23.

Castellino,F.J., Brockway,W.J., Thomas,J.K., Liano,H.T., and Rawitch,A.B. 1973. Rotational diffusion analysis of the conformational alterations produced in plasminogen by certain antifibrinolytic amino acids. *Biochemistry* **12**:2787-2791.

Chang,Y., Mochalkin,I., McCance,S.G., Cheng,B., Tulinsky,A., and Castellino,F.J. 1998. Structure and ligand binding determinants of the recombinant kringle 5 domain of human plasminogen. *Biochemistry* **37**:3258-3271.

Christensen,U. and Molgaard,L. 1991. Stopped-flow fluorescence kinetic studies of Glu-plasminogen. Conformational changes triggered by AH-site ligand binding. *FEBS Lett.* **278**:204-206.

Cockell,C.S., Marshall,J.M., Dawson,K.M., Cederholm-Williams,S.A., and Ponting,C.P. 1998. Evidence that the conformation of unliganded human plasminogen is maintained via an intramolecular interaction between the lysine-binding site of kringle 5 and the N-terminal peptide. *Biochem. J.* **333 (Pt 1)**:99-105.

Dam,L. and Schuck,P. 2004. Calculating sedimentation coefficient distributions by direct modeling of sedimentation velocity concentration profiles. *Methods in Enzymology* **384**:185-212.

Daniel,E. and Weber,G. 1966. Cooperative effects in binding by bovine serum albumin. I. The binding of 1-anilino-8-naphthalenesulfonate. Fluorimetric titrations. *Biochemistry* **5**:1893-1900.

Daniel,E. and Yang,J.T. 1973. Analysis of the circular dichroism of the complexes of 8-anilino-1-naphthalenesulfonate with bovine serum albumin. *Biochemistry* **12**:508-512.

Donate,L.E., Gherardi,E., Srinivasan,N., Sowdhamini,R., Aparicio,S., and Blundell,T.L. 1994. Molecular evolution and domain structure of plasminogen-related growth factors (HGF/SF and HGF1/MSP). *Protein Sci.* **3**:2378-2394.

Dumoulin M., Ueno H., Hayashi R., and Balny C. 1999. Contribution of the carbohydrate moiety to conformational stabiity of the carboxypeptidase Y. *Eur. J. Biochem.* **262**:475-483.

Durchschlag,H. and Jaenicke,R. 1982. Partial specific volume changes of proteins densimetric studies. *Biochem. Biophys. Res. Commun.* **108**:1074-1079.

Fehlhammer,H., Bode,W., and Huber,R. 1977. Crystal structure of bovine trypsinogen at 1-8 A resolution. II. Crystallographic refinement, refined crystal structure and comparison with bovine trypsin. *J. Mol. Biol.* **111**:415-438.

Fless,G.M., Halfman,C.J., and Kirk,E.W. 2000. The Relationship between the Effect of Lysine Analogues and Salt on the Conformation of Lipoprotein(a). *Biochemistry* **39**:2740-2747.

Fredenburgh,J.C. and Nesheim,M.E. 1992. Lys-plasminogen is a significant intermediate in the activation of Glu-plasminogen during fibrinolysis in vitro. *J. Biol. Chem.* **267**:26150-26156.

Gladysheva,I.P., Turner,R.B., Sazonova,I.Y., Liu,L., and Reed,G.L. 2003. Coevolutionary patterns in plasminogen activation. *Proc. Natl. Acad. Sci. U. S. A* **100**:9168-9172.

Kahn,P.C. 1979. The interpretation of near-ultraviolet circular dichroism. *Methods in Enzymology* **61**:339-378.

Kamen,D.E. and Woody,R.W. 2001. A partially folded intermediate conformation is induced in pectate lyase C by the addition of 8-anilino-1-naphthalenesulfonate (ANS). *Protein Sci.* **10**:2123-2130.

Kornblatt,J.A. 2000. Understanding the fluorescence changes of human plasminogen when it binds the ligand, 6-aminohexanoate: a synthesis. *Biochim. Biophys. Acta* **1481**:1-10.

Kornblatt,J.A., Kornblatt,M.J., Clery,C., and Balny,C. 1999. The effects of hydrostatic pressure on the conformation of plasminogen. *Eur. J. Biochem.* **265**:120-126.

Kornblatt,J.A., Rajotte,I., and Heitz,F. 2001. Reaction of canine plasminogen with 6-aminohexanoate: a thermodynamic study combining fluorescence, circular dichroism, and isothermal titration calorimetry. *Biochemistry* **40**:3639-3647.

Lartigue A., Guez A., Spinelli S., Riviere S., Brossut R., Tegoni M., and Cambillau C. 2003. The Crystal structure of a cockroach pheromone-binding protein suggests a new ligand binding and release mechanism. *J. Biol. Chem.* **278**:302-313.

Leavitt,S. and Freire,E. 2001. Direct measurement of protein binding energetics by isothermal titration calorimetry. *Curr. Opin. Struct. Biol.* **11**:560-566.

Lebowitz,J., Lewis,M.S., and Schuck,P. 2002. Modern analytical ultracentrifugation in protein science: a tutorial review. *Protein Sci.* **11**:2067-2079.

Llinas,M. 2004. Primary Sequence of Human Plasminogen. http://www.chem.cmu.edu/groups/Llinas/res/structure/hpk.html.

Mangel,W.F., Lin,B.H., and Ramakrishnan,V. 1990. Characterization of an extremely large, ligand-induced conformational change in plasminogen. *Science* **248**:69-73.

Markus G. 1996. Conformational changes in plasminogen, their effect on activation , and the agents that modulate activation rates - a review. *Fibrinolysis* **10**:75-85.

Markus,G., DePasquale,J.L., and Wissler,F.C. 1978. Quantitative determination of the binding of epsilon-aminocaproic acid to native plasminogen. *J. Biol. Chem.* **253**:727-732.

Marti,D.N., Schaller,J., and Llinas,M. 1999. Solution structure and dynamics of the plasminogen kringle 2-AMCHA complex: 3(1)-helix in homologous domains. *Biochemistry* **38**:15741-15755.

Masui,R. and Kuramitsu,S. 1998. Probing of DNA-binding sites of Escherichia coli RecA protein utilizing 1-anilinonaphthalene-8-sulfonic acid. *Biochemistry* **37**:12133-12143.

Mathews,I.I., Vanderhoff-Hanaver,P., Castellino,F.J., and Tulinsky,A. 1996. Crystal structures of the recombinant kringle 1 domain of human plasminogen in complexes with the ligands epsilon-aminocaproic acid and trans-4-(aminomethyl)cyclohexane-1-carboxylic Acid. *Biochemistry* **35**:2567-2576.

Matulis,D., Baumann,C.G., Bloomfield,V.A., and Lovrien,R.E. 1999. 1-anilino-8-naphthalene sulfonate as a protein conformational tightening agent. *Biopolymers* **49**:451-458.

MicroCal™ Inc. ITC Data Analysis in Origin®. 5. 1998.
Ref Type: Pamphlet

Miles,L.A., Castellino,F.J., and Gong,Y. 2003. Critical role for conversion of glu-plasminogen to Lys-plasminogen for optimal stimulation of plasminogen activation on cell surfaces. *Trends Cardiovasc. Med.* **13**:21-30.

Miyashita,C., Wenzel,E., and Heiden,M. 1988. Plasminogen: a brief introduction into its biochemistry and function. *Haemostasis* **18 Suppl 1**:7-13.

Mulichak,A.M., Tulinsky,A., and Ravichandran,K.G. 1991. Crystal and molecular structure of human plasminogen kringle 4 refined at 1.9-A resolution. *Biochemistry* **30**:10576-10588.

Nieuwenhuizen,W. 2001. Fibrin-mediated plasminogen activation. *Ann. N. Y. Acad. Sci.* **936**:237-246.

Ohyama,S., Harada,T., Chikanishi,T., Miura,Y., and Hasumi,K. 2004. Nonlysine-analog plasminogen modulators promote autoproteolytic generation of plasmin(ogen) fragments with angiostatin-like activity. *Eur. J. Biochem.* **271**:809-820.

Ory,J.J. and Banaszak,L.J. 1999. Studies of the ligand binding reaction of adipocyte lipid binding protein using the fluorescent probe 1, 8-anilinonaphthalene-8-sulfonate. *Biophys. J.* 77:1107-1116.

Parry,M.A., Zhang,X.C., and Bode,I. 2000. Molecular mechanisms of plasminogen activation: bacterial cofactors provide clues. *Trends Biochem. Sci.* **25**:53-59.

Peisach E., Wang J., de los Santos T., Reich E., and Ringe D. 1999. Crystal Structure of the Proenzyme Domain of Plasminogen. *Biochemistry* **38**:11180-11188.

Pirie-Shepherd,S.R., Coffman,K.T., Resnick,D., Chan,R., Kisker,O., Folkman,J., and Waters,D.J. 2002. The role of angiostatin in the spontaneous bone and prostate cancers of pet dogs. *Biochem. Biophys. Res. Commun.* **292**:886-891.

Ploug,M., Ellis,V., and Dano,K. 1994. Ligand interaction between urokinase-type plasminogen activator and its receptor probed with 8-anilino-1-naphthalenesulfonate. Evidence for a hydrophobic binding site exposed only on the intact receptor. *Biochemistry* **33**:8991-8997.

Ponting,C.P., Holland,S.K., Cederholm-Williams,S.A., Marshall,J.M., Brown,A.J., Spraggon,G., and Blake,C.C. 1992. The compact domain conformation of human Glu-plasminogen in solution. *Biochim. Biophys. Acta* **1159**:155-161.

Ptitsyn,O.B. 1987. *J. Protein Chem.* **6**:273-293.

Schaller,J., Moser,P.W., nnegger-Muller,G.A., Rosselet,S.J., Kampfer,U., and Rickli,E.E. 1985. Complete amino acid sequence of bovine plasminogen. Comparison with human plasminogen. *Eur. J. Biochem.* **149**:267-278.

Schaller,J. and Rickli,E.E. 1988. Structural aspects of the plasminogen of various species. *Enzyme* **40**:63-69.

Schaller,J., Straub,C., Kampfer,U., and Rickli,E.E. 1989. Complete amino acid sequence of canine miniplasminogen. *Protein Seq. Data Anal.* **2**:445-450.

Schonbrunn,E., Eschenburg,S., Luger,K., Kabsch,W., and Amrhein,N. 2000. Structural basis for the interaction of the fluorescence probe 8-anilino-1-naphthalene sulfonate (ANS) with the antibiotic target MurA. *Proc. Natl. Acad. Sci. U. S. A* **97**:6345-6349.

Schuck,P. 1998. Sedimentation analysis of noninteracting and self associating solutes using numerical solutions to the Lamm equation. *Biophysical Journal* **75**:1503-1512.

Seale,J.W., Martinez,J.L., and Horowitz,P.M. 1995. Photoincorporation of 4,4'-bis(1-anilino-8-naphthalenesulfonic acid) into the apical domain of GroEL: specific information from a nonspecific probe. *Biochemistry* **34**:7443-7449.

Shi,L., Palleros,D.R., and Fink,A.L. 1994. Protein conformational changes induced by 1,1'-bis(4-anilino-5-naphthalenesulfonic acid): preferential binding to the molten globule of DnaK. *Biochemistry* **33**:7536-7546.

Sodeinde,O.A. and Goguen,J.D. 1989. Nucleotide sequence of the plasminogen activator gene of Yersinia pestis: relationship to ompT of Escherichia coli and gene E of Salmonella typhimurium. *Infect. Immun.* **57**:1517-1523.

Soldeinde O.A. and Goguen J.D. Nucleotide Sequence of the Plasminogen Activator Gene of *Yersinia pestis*: Relationship to the *omp*T of *Escherichia coli* and Gene E of *Salmonella typhimurium*. Infection and Immunity 57[5], 1517-1523. 1989.
Ref Type: Generic

Sottrup-Jensen,L., Claeys,M., Zajdel M, Petersen,T., and Magnusson S 1978. The Primary Structure of Human Plasminogen: Isolation of Two Lysine-Binding Fragments and One "Mini-" Plasminogen (MW, 38,000) by Elastase-Catalyzed-Specific Limited Proteolysis. *Progress in Chemical Fibrinolysis and Thrombosis* **3**:191-209.

Stryer L.S. 1965. *J. Mol. Bio.* **13**:482-495.

Sugawara,Y., Takada,Y., and Takada,A. 1984. Fluorescence polarization and spectropolarimetric studies on the conformational changes induced by omega-aminoacids in two isozymes of Glu-plasminogen (I and II). *Thromb. Res.* **33**:269-275.

Takada,A. and Takada,Y. 1988. Physiology of plasminogen: with special reference to activation and degradation. *Haemostasis* **18 Suppl 1**:25-35.

Terzyan,S., Wakeham,N., Zhai,P., Rodgers,K., and Zhang,X.C. 2004. Characterization of Lys-698 to met substitution in human plasminogen catalytic domain. *Proteins* **56**:277-284.

Tranqui L., Prandini M.H., and Chapel A. 1979. The structure of Plasminogen studied by electron microscopy. *Biologie Cellul* **34**:39-42.

Urano,T., Sator,d.S., V, Chibber,B.A., and Castellino,F.J. 1987. The control of the urokinase-catalyzed activation of human glutamic acid 1-plasminogen by positive and negative effectors. *J. Biol. Chem.* **262**:15959-15964.

Uversky,V.N., Winter,S., and Lober,G. 1998. Self-association of 8-anilino-1-naphthalene-sulfonate molecules: spectroscopic characterization and application to the investigation of protein folding. *Biochim. Biophys. Acta* **1388**:133-142.

Wallen,P. 1978. Chemistry of Plasminogen and Plasminogen Activation. *Progress in Chemical Fibrinolysis and Thrombosis* **3**:167-181.

Wang,X., Terzyan,S., Tang,J., Loy,J.A., Lin,X., and Zhang,X.C. 2000. Human plasminogen catalytic domain undergoes an unusual conformational change upon activation. *J. Mol. Biol.* **295**:903-914.

Weber,G. and Daniel,E. 1966. Cooperative effects in binding by bovine serum albumin. II. The binding of 1-anilino-8-naphthalenesulfonate. Polarization of the ligand fluorescence and quenching of the protein fluorescence. *Biochemistry* **5**:1900-1907.

Weber,L.D., Tulinsky,A., Johnson,J.D., and El-Bayoumi,M.A. 1979. Expression of functionality of alpha-chymotrypsin. The structure of a fluorescent probe--alpha-chymotrypsin complex and the nature of its pH dependence. *Biochemistry* **18**:1297-1303.

Wesiel J.W., Nagaswami C., Korsholm B., Petersen L.C., and Suenson E. 1984. Interactions of Plasminogen with polymerizing fibrin and its derivatives, monitored with a photoaffinity cross-linker and electron microscopy. *J. Molec. Biol.* **235**:1117-1135.

Wohl,R.C., Sinio,L., Summaria,L., and Robbins,K.C. 1983. Comparative activation kinetics of mammalian plasminogens. *Biochim. Biophys. Acta* **745**:20-31.

Wu,T.P., Padmanabhan,K., Tulinsky,A., and Mulichak,A.M. 1991. The refined structure of the epsilon-aminocaproic acid complex of human plasminogen kringle 4. *Biochemistry* **30**:10589-10594.